

A Diffeomorphism Groupoid and Algebroid Framework for Discontinuous Image Registration

March 13, 2026

LILI BAO¹, BIN XIAO², SHIHUI YING^{3, 4} AND STEFAN SOMMER¹

¹Department of Computer Science, University of Copenhagen
Universitetsparken 1, Copenhagen 2100, Denmark

²Institute for Medical Imaging Technology, Ruijin Hospital, Shanghai 201800, China

³Shanghai Institute of Applied Mathematics and Mechanics, Shanghai University, Shanghai 200444, China

⁴School of Mechanics and Engineering Science, Shanghai University, Shanghai, 200444, China

Abstract

In this paper, we propose a novel mathematical framework for piecewise diffeomorphic image registration that involves discontinuous sliding motion using a diffeomorphism groupoid and algebroid approach. The traditional Large Deformation Diffeomorphic Metric Mapping (LDDMM) registration method builds on Lie groups, which assume continuity and smoothness in velocity fields, limiting its applicability in handling discontinuous sliding motion. To overcome this limitation, we extend the diffeomorphism Lie groups to a framework of discontinuous diffeomorphism Lie groupoids, allowing for discontinuities along sliding boundaries while maintaining diffeomorphism within homogeneous regions. We provide a rigorous analysis of the associated mathematical structures, including Lie algebroids and their duals, and derive specific Euler-Arnold equations to govern optimal flows for discontinuous deformations. Some numerical tests are performed to validate the efficiency of the proposed approach.

Keywords: Lie groupoids, vortex sheet, image registration, discontinuous deformations, diffeomorphism

1 Introduction

Image registration is a fundamental and crucial technique in computer vision and medical image processing. The aim of image registration is to find reasonable spatial deformations between two or more images [26, 33]. In many applications, maintaining the integrity and consistency of structures is essential, making diffeomorphic deformations highly desirable [21]. The Large Deformation Diffeomorphic Metric Mapping (LDDMM) framework plays an important

Funding: The work of the third author was supported by the National Natural Science Foundation of China (No. 12531019). The fourth author was supported by the Novo Nordisk Foundation grants NNF18OC0052000, NNF24OC0093490 and NNF24OC0089608, the VIL-LUM FONDEN research grant 40582 and UCPH Data+ Strategy 2023 funds for interdisciplinary research.

role in such diffeomorphic registration as it provides good registration results along with a solid mathematical foundation allowing meaningful statistics to be computed on the registration results [7, 31].

However, challenges arise when encountering discontinuous deformations, such as the discontinuous sliding motion observed between lung tissues and surrounding structures during breathing [4, 5]. Registration of lungs is an essential part in medical imaging, for example for motion estimation and tumor radiotherapy. The LDDMM method, being designed for smooth and continuous deformations, struggles to capture these discontinuous movements.

To address this limitation, we propose to use the mathematical theory proposed by Izosimov and Khesin [1, 16] to model such discontinuous image registration, thereby extending the diffeomorphism group representation of deformation to a more general groupoid based framework. In our framework, discontinuities along sliding hypersurfaces are naturally handled using the structure of Lie groupoids and algebroids, while maintaining diffeomorphism in homogeneous regions. Specifically, we construct a discontinuous diffeomorphism groupoid $\text{DDiff}(M) \rightrightarrows V(M)$ to describe discontinuous deformations. We also explore the associated mathematical structures including Lie algebroids $\text{DVect}(M)$ and their duals $\text{DVect}(M)^*$, and formulate specific Euler-Arnold equations for optimal flows to drive the discontinuous deformation. The framework and examples of its effect on discontinuous image registration are illustrated in Figure 1.

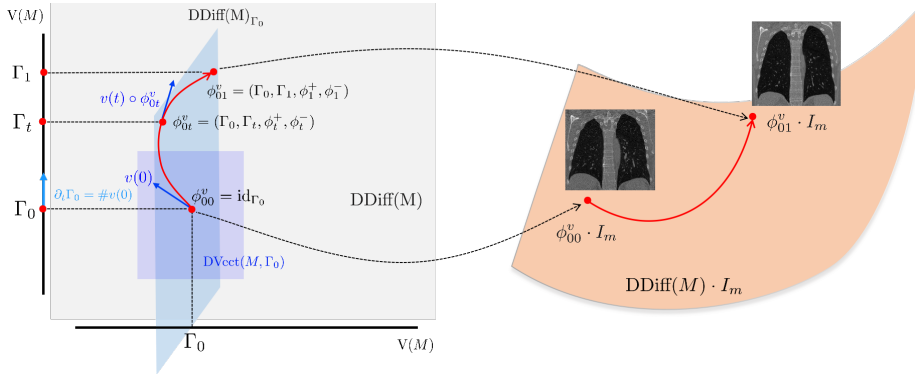


Figure 1: Illustration of the discontinuous image registration based on Lie groupoid and algebroid. (left) Illustration of the geodesic flow on groupoids $\text{DDiff}(M) \rightrightarrows V(M)$ of discontinuous diffeomorphisms with respect to the metric $\langle \cdot, \cdot \rangle_{\text{DVect}(M)}$, governed by the Euler-Arnold equation (3.37). (right) The action of discontinuous diffeomorphism groupoid on the moving image I_m .

1.1 Related work

Over the years, researchers have explored various approaches to tackle the challenge of sliding motion registration. These methods can generally be divided into two categories: displacement-based methods and velocity-based methods, both of which focus on developing elaborate regularization constraints on deformations.

Various special regularizations based on displacement fields have been pro-

posed to deal with discontinuous deformation. For example, total variation (TV) has been used to describe the discontinuity of the deformation field in [12]. To balance the smoothness and discontinuity of the deformation field across different image regions, the modified total variation (MTV) method has been proposed in [9]. Recently a time multiscale regularization strategy has been proposed in [4] to capture finer scale deformations and preserve sharper structures in images. Direction-dependent regularization methods have been employed in [13, 30], where the deformation field is decomposed into normal and tangential directions and regularized separately.

Velocity-based methods model the deformation field through a flow generated by a velocity field, as in the case of diffeomorphic frameworks like the Large Deformation Diffeomorphic Metric Mapping (LDDMM). To adapt velocity-based approaches for sliding motions, researchers have introduced specialized regularization techniques, such as decomposing the velocity fields into tangential and normal components [28, 29], and introducing a shear strain rate to control the amount of shear to approximate sliding motion in [20]. More recently, an extension of LDDMM has been proposed that incorporates both zeroth- and first-order momenta with a non-differentiable kernel, offering a novel approach to handling sliding motion [5]. All these methods have shown promise in modeling sliding motion, but a unified framework for discontinuous image registration remains elusive.

This motivates the need for a more general and mathematically rigorous framework that can naturally model discontinuities while preserving the desirable properties of diffeomorphisms in homogeneous regions. In this work, we address these challenges by introducing a groupoid-based framework for discontinuous image registration.

This work is inspired by the seminal developments in fluid dynamics and geometric mechanics in the works of Izosimov and Khesin [1, 16, 18]. Their framework, which introduces discontinuous flows and vortex sheet groupoids in the context of incompressible fluid dynamics, serves as the mathematical foundation for our proposed approach. Our paper has two primary aims: first, extending the groupoid framework to handle compressible cases needed for registration; and second, applying this extended theory to image registration, enabling the modeling of discontinuous deformations. For clarity and consistency, we follow the notation and conventions introduced in [16].

1.2 Content and outline

The organization of the paper is as follows. In Section 2, we briefly review some mathematical background of the proposed framework, including the LDDMM approach to image registration and Lie groupoids and Lie algebroid. In Section 3, the detailed formulation of the proposed framework is explained, we first describe the concept of discontinuous diffeomorphism groupoid and the associated mathematical structures including Lie algebroids of discontinuous vector fields and their duals. Following this, we derive the Euler-Arnold equations for optimal flows in the present context. Then we show how the proposed groupoid representation can be used for discontinuous image registration problems. In Section 4, we explore the applications of the proposed framework to image registration. We conclude the paper and discuss possible future works in Section 5. The paper thus has the following contributions:

1. We show how Lie groupoids can be used in shape analysis to model piecewise diffeomorphic transformations, and we provide a detailed account of the theoretical foundation.
2. We derive the Euler-Poincaré equations on Lie groupoids with general inertia operators in the compressible case, extending the traditional EPDiff equations as used in shape analysis from Lie groups to Lie groupoids.
3. We show how the proposed framework can be used for discontinuous image registration with numerical schemes, ensuring that diffeomorphisms are preserved across different regions while allowing for discontinuities along a hypersurface for modeling sliding motion.

2 Mathematical Background

In this section, we review some basic mathematical concepts relevant to this work, including the well-known LDDMM registration method and concepts from Lie groupoids theory.

2.1 LDDMM registration

We begin by briefly reviewing the LDDMM approach, which has a solid mathematical foundation through the use of Lie groups. A detailed treatment can be found in [36], and with a perspective from fluid dynamics in [2, 19]. The problem of image registration based on diffeomorphisms can be described as follows: Given two images I_m and I_f defined on image domain $\Omega \subset \mathbb{R}^d$, where I_m is the moving image and I_f is the fixed image, we aim to find a reasonable diffeomorphic deformation $\phi : \Omega \rightarrow \mathbb{R}^d$ such that the fixed image I_f and the deformed moving image $I_m^* = \phi \cdot I_m$ are as closely as possible, i.e., $I_f \approx \phi \cdot I_m = I_m \circ \phi^{-1}$ (see Figure 2). Additionally, we hope such a ϕ to be as simple as possible, i.e. as close as possible to the identity deformation. Based on this, the mathematical formulation of the registration problem can be given as:

$$\phi^* = \arg \min_{\phi} E(\phi) := E_S(\phi \cdot I_m, I_f) + E_R(\phi), \quad (2.1)$$

where the first term $E_S(\phi \cdot I_m, I_f)$ is the similarity term that measures the similarity between the two images, and the second term $E_R(\phi)$ is the regularization term, ensuring the smoothness of the deformation field.

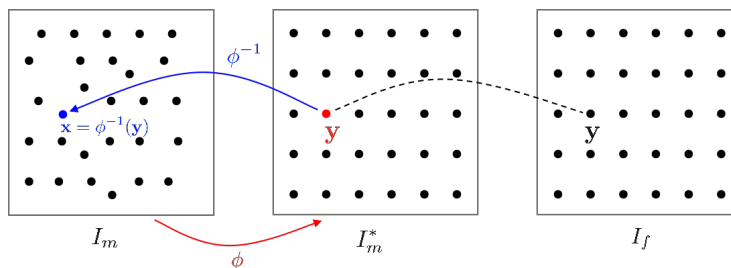


Figure 2: An illustration of image registration.

In the LDDMM method, it is assumed that the deformation $\phi = \phi_{01}^v$ is obtained as the endpoint of a flow generated by a time-dependent velocity field $v(t)$, guided by the following differential equation [11, 27]:

$$\frac{\partial \phi(t, x)}{\partial t} = v(t, \phi(t, x)), \quad \phi(0, x) = x, \quad \forall x \in \Omega, \quad (2.2)$$

achieving registration between the two images. To ensure that the deformation field is as simple and smooth as possible, and close to the identity deformation, the regularization term $E_R(\phi)$ can be defined using the distance given as follows [32, 36]:

$$E_R(\phi) = d_V^2(\text{Id}, \phi) = \min_{v(t) \in V, \phi_{01}^v = \phi} \int_0^1 \|v(t)\|_V^2 dt. \quad (2.3)$$

The velocity v lies in the admissible Hilbert space V with associated norm $\|\cdot\|_V$, and V is usually produced by using a differential operator \mathcal{I} [6]. The inner product is defined as follows:

$$\langle u, v \rangle_V := \langle \mathcal{I}u, v \rangle_{L^2} = \langle u, \mathcal{I}v \rangle_{L^2}, \quad (2.4)$$

where $\langle \cdot, \cdot \rangle_{L^2}$ is the L^2 inner product of square-integrable vector fields on Ω . This induces the norm $\|v\|_V := \sqrt{\langle v, v \rangle_V}$. Let $\text{Diff}(\Omega)$ denote the Lie group of smooth diffeomorphism on Ω , then the set of flow at time 1 built from V denoted by G_V is a subgroup of $\text{Diff}(\Omega)$, and is a Lie group [36]. The tangent space of G_V at the identity deformation is the space $V = \text{Vect}(\Omega)$ of smooth vector fields on Ω [19]. Figure 3 illustrates the LDDMM registration framework.

In fact, the operator \mathcal{I} is also the dual operator between the space V and its dual space V^* , $\mathcal{I} : V \rightarrow V^*$. The operator \mathcal{I} is also referred to as the momentum operator. This is because \mathcal{I} relates the inner product on V to the L^2 inner product, and the image of the element v under the operator \mathcal{I} , denoted as $\mathcal{I}v$, is called the momentum, denoted as m , i.e., $m = \mathcal{I}v$. In fluid dynamics, the momentum operator is also commonly referred to as the inertia operator [2].

Minimizing the functional in (2.1) with the regularizer in (2.3) yields a geodesic with the shortest length path in G_V , uniquely determined by integrating the Euler-Poincaré differential equations on the diffeomorphism group (EPDiff) with an initial condition [23, 36]:

$$\frac{\partial m(t)}{\partial t} + v(t) \cdot \nabla m(t) + (\nabla v(t))^T \cdot m(t) + m(t)(\text{div } v(t)) = 0, \quad (2.5)$$

$$v(t) = K * m(t). \quad (2.6)$$

That is, given an optimal initial momentum $m(0)$, according to the time evolution of momentum (2.5) and the connection between momentum and velocity (2.6), the entire path of velocities $v(t)$ can be recovered, and the corresponding optimal deformation φ also can be reconstructed via equation (2.2). See e.g. [36] for more details.

For the convenience of subsequent discussions, we describe an equivalent form of the EPDiff equation [22, 25]. Instead of considering the momentum $m(t)$ a vector field, it can be considered a differential form. Let \tilde{m} be a 1-form density [14, 15]:

$$\tilde{m} = m \otimes \mu = \sum_i m_i dx_i \otimes (dx_1 \wedge \cdots \wedge dx_n),$$

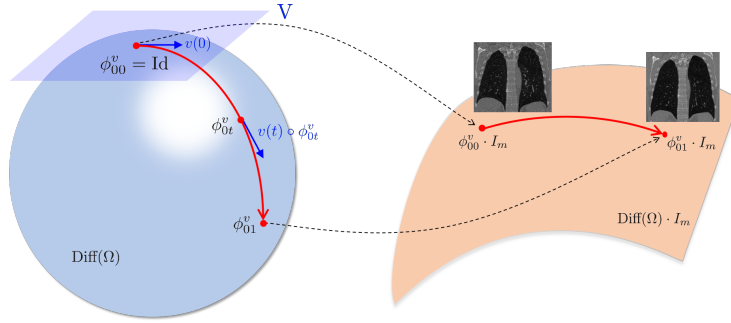


Figure 3: (left) Illustration of the geodesic flow on groups $\text{Diff}(\Omega)$ of diffeomorphisms with respect to the right-invariant metric $\langle \cdot, \cdot \rangle_{\text{Vect}(\Omega)}$. (right) The action of the diffeomorphism group on the moving image I_m .

It is not difficult to verify that EPDiff (2.5) is equivalent to

$$\partial_t \tilde{m}(t) + \mathcal{L}_{v(t)} \tilde{m}(t) = 0, \quad (2.7)$$

where $\mathcal{L}_{v(t)} \tilde{m}(t)$ denotes the Lie derivative of the 1-form density \tilde{m} along the vector field $v(t)$.

2.2 Lie groupoid and Lie algebroid

We now give a brief overview of Lie groupoids and their associated Lie algebroids, which will form the foundation for the framework in the next section. More details can be found in [10, 16].

Definition 2.1 (Groupoid [16]). *A groupoid $\mathcal{G} \rightrightarrows B$ consists of a pair of sets, where B is the set of objects and \mathcal{G} is the set of arrows, equipped with the following structure:*

1. *There are two maps, src and $\text{trg} : \mathcal{G} \rightarrow B$, called the source and target maps.*
2. *There is a partially defined binary operation on \mathcal{G} , $(g, h) \mapsto gh$, defined for all $g, h \in \mathcal{G}$ such that $\text{src}(g) = \text{trg}(h)$, and it satisfies the following properties:*

- (a) $\text{src}(gh) = \text{src}(h)$, $\text{trg}(gh) = \text{trg}(g)$.
- (b) *Associativity: $g(hk) = (gh)k$ whenever these expressions are defined.*
- (c) *Identity: For each $x \in B$, there exists an element $\text{id}_x \in \mathcal{G}$ such that $\text{src}(\text{id}_x) = \text{trg}(\text{id}_x) = x$ and for every $g \in \mathcal{G}$, $\text{id}_{\text{trg}(g)} \cdot g = g \cdot \text{id}_{\text{src}(g)} = g$.*
- (d) *Inverse: For each $g \in \mathcal{G}$, there exists an element $g^{-1} \in \mathcal{G}$ such that $\text{src}(g^{-1}) = \text{trg}(g)$, $\text{trg}(g^{-1}) = \text{src}(g)$, $g^{-1}g = \text{id}_{\text{src}(g)}$, and $gg^{-1} = \text{id}_{\text{trg}(g)}$.*

The structure of a groupoid, along with its inverses, identities, and multiplication operations, is illustrated in Figure 4. In this diagram, the groupoid

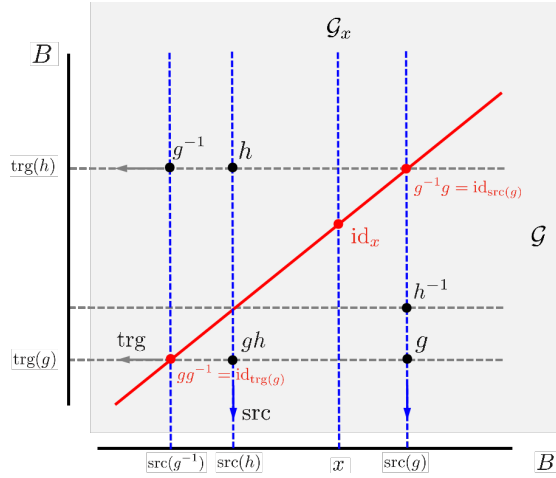


Figure 4: The structure of a groupoid $\mathcal{G} \rightrightarrows B$.

$\mathcal{G} \rightrightarrows B$ is represented as a square. The vertical projection represents the source map $\text{src} : \mathcal{G} \rightarrow B$, while the horizontal projection represents the target map $\text{trg} : \mathcal{G} \rightarrow B$. Elements on the diagonal where $\text{src} = \text{trg}$ consist of all the identity elements in \mathcal{G} . A pair of inverse elements is symmetric with respect to this diagonal.

Definition 2.2 (Lie groupoid [16]). *A groupoid $\mathcal{G} \rightrightarrows B$ is called a Lie groupoid if both \mathcal{G} and B are manifolds, the source and target maps are submersions, and the multiplication, identity, and inversion maps are smooth.*

Definition 2.3 (Lie algebroid [16]). *A Lie algebroid $\mathcal{A} \rightarrow B$ is a vector bundle \mathcal{A} over a manifold B , equipped with a Lie bracket $[\cdot, \cdot]$ on its smooth sections and a vector bundle map $\# : \mathcal{A} \rightarrow TB$, called the anchor map, such that for any smooth sections ζ, η of \mathcal{A} and any smooth function f on B , the following identity holds:*

$$[\zeta, f\eta] = f[\zeta, \eta] + (\mathcal{L}_{\#\zeta}f)\eta.$$

Here, B is called the base manifold, TB is the tangent bundle of B , and $\#$ is the anchor map.

3 Lie Groupoids for Discontinuous Image Registration

The LDDMM registration method based on Lie group theory treats smooth, continuous registration as a problem of smooth, continuous flow. To describe the discontinuous registration problem with sliding boundaries, we can treat it as a discontinuous flow problem involving vortex sheets, where the flow velocity exhibits discontinuous jumps at the vortex sheets. We will present the main contribution of this paper in this section: introducing the use of discontinuous diffeomorphism groupoid in shape analysis and image registration thereby allowing for discontinuities along hypersurfaces, and the associated mathematical

structures including Lie algebroids and their duals, and meanwhile giving the framework for discontinuous image registration using the proposed theory.

Our work builds upon the mathematical framework established by Izosimov and Khesin in [16, 18] for modeling vortex sheets in incompressible fluid flows, which relies on the Lie groupoid $\text{DSDiff}(M)$ of discontinuous volume-preserving diffeomorphisms and the Lie algebroid $\text{DSVect}(M)$ of divergence-free discontinuous vector fields. On the mathematical side, the novelty of our work lies in extending the framework to the compressible case by using the Lie groupoid $\text{DDiff}(M)$ of discontinuous diffeomorphisms and the Lie algebroid $\text{DVect}(M)$ of discontinuous vector fields, without imposing the volume-preserving and divergence-free conditions. In this extended setting, the associated structures are modified accordingly to accommodate compressibility while preserving the fundamental geometric framework.

We closely follow the structural framework established in [16, Section 6], maintaining the formulation of key mathematical constructs within our extended setting. To this end, we consider an n -dimensional Riemannian manifold M equipped with a Riemannian volume form μ . In the next subsection, we will describe the Lie groupoid $\text{DDiff}(M)$ and its associated structures.

3.1 The Lie groupoid of discontinuous diffeomorphisms

Let $\Gamma_0 \subset M$ be a hypersurface (often referred to as a vortex sheet) that divides M into two regions, $D_{\Gamma_0}^+$ and $D_{\Gamma_0}^-$, such that $M = D_{\Gamma_0}^+ \cup \Gamma_0 \cup D_{\Gamma_0}^-$.

We begin by defining the full groupoid of discontinuous diffeomorphisms. This groupoid consists of all diffeomorphisms discontinuous along a hypersurface, i.e. all quadruples $(\Gamma_1, \Gamma_2, \phi^+, \phi^-)$, where Γ_1 and Γ_2 are hypersurfaces in M , each an image of Γ_0 under some diffeomorphism of M , and $\phi^\pm : D_{\Gamma_1}^\pm \rightarrow D_{\Gamma_2}^\pm$ are diffeomorphisms, where $M = D_{\Gamma_i}^+ \cup \Gamma_i \cup D_{\Gamma_i}^-$ for $i = 1, 2$. The groupoid structure is equipped with source and target maps: the source of $(\Gamma_1, \Gamma_2, \phi^+, \phi^-)$ is $\text{src}(\Gamma_1, \Gamma_2, \phi^+, \phi^-) = \Gamma_1$ and the target of $(\Gamma_1, \Gamma_2, \phi^+, \phi^-)$ is $\text{trg}(\Gamma_1, \Gamma_2, \phi^+, \phi^-) = \Gamma_2$. The composition is defined as follows:

$$(\Gamma_2, \Gamma_3, \psi^+, \psi^-)(\Gamma_1, \Gamma_2, \phi^+, \phi^-) = (\Gamma_1, \Gamma_3, \psi^+ \phi^+, \psi^- \phi^-). \quad (3.1)$$

The base space of the full groupoid of discontinuous diffeomorphisms is the set of images of Γ_0 under diffeomorphisms in $\text{Diff}(M)$.

In this work, we do not study the full groupoid described above. Instead, we focus on a subgroupoid with additional regularity constraints. Specifically, we require that the diffeomorphisms ϕ^+ and ϕ^- belong to the subgroup $G_V \subset \text{Diff}(M)$. This regularity condition ensures that ϕ^+ and ϕ^- are at least continuously differentiable. For convenience, we denote this subgroupoid as $\text{DDiff}(M)$. The base space of the $\text{DDiff}(M)$ thus is defined as follows:

$$V(M) = \{\Gamma = \phi(\Gamma_0) \mid \phi \in G_V\}. \quad (3.2)$$

Elements of $\text{DDiff}(M)$ are thus quadruples $(\Gamma_1, \Gamma_2, \phi^+, \phi^-)$ satisfying the above regularity, with the source and target maps, along with the composition operation (illustrated in Figure 5) inherited from the full groupoid.

Definition 3.1. *The source fiber of $\text{DDiff}(M)$ corresponding to $\Gamma \in V(M)$ is the set $\text{DDiff}(M)_\Gamma = \{\phi \in \text{DDiff}(M) \mid \text{src}(\phi) = \Gamma\}$.*

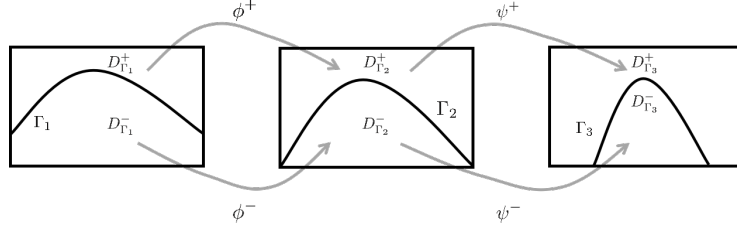


Figure 5: Illustration of the composition rule of two groupoid elements $(\Gamma_1, \Gamma_2, \phi^+, \phi^-)$ and $(\Gamma_2, \Gamma_3, \psi^+, \psi^-)$ in the Lie groupoid $\text{DDiff}(M)$, resulting in $(\Gamma_1, \Gamma_3, \psi^+\phi^+, \psi^-\phi^-)$.

Theorem 3.2. $\text{DDiff}(M) \rightrightarrows V(M)$ is a Lie groupoid.

Proof. It is straightforward to verify that it satisfies each condition in the definition of a groupoid as given in Definition 2.1, and thus it is a groupoid. To further prove that it is a Lie groupoid, refer to page 476 of [16]. \square

Figure 6 illustrates the structure of the Lie groupoid $\text{DDiff}(M) \rightrightarrows V(M)$. In this diagram, the Lie groupoid $\text{DDiff}(M) \rightrightarrows V(M)$ is represented as a cube. The vertical projection represents the source map $\text{src} : \text{DDiff}(M) \rightarrow V(M)$, and the horizontal projection represents the target map $\text{trg} : \text{DDiff}(M) \rightarrow V(M)$. Each element Γ in $V(M)$ corresponds to an identity element $\text{id}_\Gamma = (\Gamma, \Gamma, \text{id})$ in $\text{DDiff}(M)$. The diagonal where $\text{src} = \text{trg}$ consists of all identity elements in $\text{DDiff}(M)$. The source fiber $\text{DDiff}(M)_\Gamma$ can be visualized as a vertical plane passing through Γ , indicating that the source map value at every point on this plane is Γ .

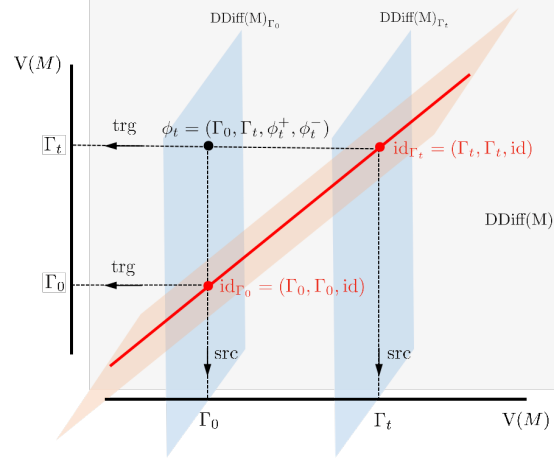


Figure 6: The structure of the Lie groupoid $\text{DDiff}(M) \rightrightarrows V(M)$.

3.2 The Lie algebroid of discontinuous vector fields

In this subsection, we introduce the Lie algebroid $\text{DVect}(M) \rightarrow V(M)$ corresponding to the Lie groupoid $\text{DDiff}(M) \rightrightarrows V(M)$.

For the sake of convenience, we first define several spaces of tensor fields that are discontinuous along the vortex sheet Γ . All such tensor fields are assumed to have the form $\chi_\Gamma^+ \xi^+ + \chi_\Gamma^- \xi^-$, where χ_Γ^\pm are the characteristic functions of D_Γ^\pm , and ξ^\pm are smooth within D_Γ^\pm up to the boundary Γ . The following spaces are defined:

$$\begin{aligned} \text{DC}^\infty(M, \Gamma) &= \{\chi_\Gamma^+ f^+ + \chi_\Gamma^- f^- \mid f^\pm \in C^\infty(D_\Gamma^\pm)\} && \text{(discontinuous functions)} \\ \text{DVect}'(M, \Gamma) &= \{\chi_\Gamma^+ v^+ + \chi_\Gamma^- v^- \mid v^\pm \in \text{Vect}(D_\Gamma^\pm)\} && \text{(discontinuous vector fields)} \\ \text{D}\Omega^1(M, \Gamma) &= \{\chi_\Gamma^+ m^+ + \chi_\Gamma^- m^- \mid m^\pm \in \Omega^1(D_\Gamma^\pm)\} && \text{(discontinuous 1-forms)} \\ \text{DDense}(M, \Gamma) &= \{\chi_\Gamma^+ \mu^+ + \chi_\Gamma^- \mu^- \mid \mu^\pm \in \text{Dense}(D_\Gamma^\pm)\} && \text{(discontinuous densities)} \end{aligned}$$

Here, $\text{Dense}(D_\Gamma^\pm)$ denotes the space of smooth densities on D_Γ^\pm . For the space of discontinuous vector fields $\text{DVect}'(M, \Gamma)$, there is a special subspace of discontinuous vector fields $\text{DVect}(M, \Gamma)$, where the normal components of the vector fields u^+ and u^- are continuous across the boundary Γ :

$$\text{DVect}(M, \Gamma) := \{\chi_\Gamma^+ u^+ + \chi_\Gamma^- u^- \mid u^\pm \in \text{Vect}(D_\Gamma^\pm), u^+|_\Gamma - u^-|_\Gamma \text{ is tangent to } \Gamma\}.$$

Then we recall the regularized version $\mathcal{D}^\mathcal{R}$ of the differential operator \mathcal{D} on discontinuous tensor fields ξ , as introduced in [16]: $\mathcal{D}^\mathcal{R}\xi = \chi_\Gamma^+ \mathcal{D}\xi^+ + \chi_\Gamma^- \mathcal{D}\xi^-$, which allows \mathcal{D} to operate on discontinuous tensor fields by applying the differential operator on each side of the discontinuity separately and then combining the results accordingly.

For a function $f = \chi_\Gamma^+ f^+ + \chi_\Gamma^- f^- \in \text{DC}^\infty(M, \Gamma)$, the jump across the hypersurface Γ is defined as $\text{jump}(f) = f^+|_\Gamma - f^-|_\Gamma$. Below, we present two fundamental lemmas concerning operations on discontinuous functions, adapted from [16], which are essential to the subsequent proof. The first lemma is a key result from [16, Lemma 5.2], stated as follows:

Lemma 3.3 ([16]). *Let $\Gamma_t \in \text{VS}(M)$ be a family of hypersurfaces parametrized by $t \in \mathbb{R}$, $f_t \in \text{DC}^\infty(M, \Gamma_t)$ be a smooth family of functions discontinuous across Γ_t , then*

$$\frac{d}{dt} \int_M f_t \mu = \int_M \frac{d^\mathcal{R} f_t}{dt} \mu + \int_{\Gamma_t} \text{jump}(f_t) \frac{d\Gamma_t}{dt}. \quad (3.3)$$

This result, originally formulated for $\Gamma_t \in \text{VS}(M)$, extends to $\Gamma_t \in \text{V}(M)$. The second lemma is a slight modification of [16, Lemma 5.4], as we no longer assume the divergence-free condition $\text{div } v^\pm = 0$.

Lemma 3.4. *Let $f \in \text{DC}^\infty(M, \Gamma)$, and let $v \in \text{DVect}(M, \Gamma)$. Then*

$$\int_M \mathcal{L}_v^\mathcal{R}(f\mu) = \int_M (\mathcal{L}_v^\mathcal{R} f)\mu + \int_M \text{div}^\mathcal{R}(v) f\mu = \int_\Gamma \text{jump}(f) i_v \mu. \quad (3.4)$$

Proof.

$$\begin{aligned} \int_M \mathcal{L}_v^\mathcal{R}(f\mu) &= \int_{D_\Gamma^+} \mathcal{L}_v(f\mu) + \int_{D_\Gamma^-} \mathcal{L}_v(f\mu) \\ \int_{D_\Gamma^+} \mathcal{L}_v(f\mu) &= \int_{D_\Gamma^+} (\mathcal{L}_v f)\mu + \text{div}(v) f\mu = \int_{D_\Gamma^+} i_v df\mu + f di_v \mu \end{aligned}$$

$$= \int_{D_\Gamma^+} d(fi_v\mu) = \int_{\partial D_\Gamma^+} fi_v\mu$$

Since for $\alpha \in \Omega^1(M)$, $\mu \in \Omega^n(M)$, $v \in \text{Vect}(M)$, we have [2]

$$\alpha \wedge i_v\mu = \langle \alpha, v \rangle \mu = i_v\alpha\mu, d(fw) = fd(w) + d(f) \wedge w.$$

Then the third equation arise from

$$\int_{D_\Gamma^+} d(fi_v\mu) = \int_{D_\Gamma^+} fdi_v\mu + df \wedge i_v\mu = \int_{D_\Gamma^+} fdi_v\mu + i_vdf\mu$$

and the last equation comes from the Stokes formula.

Analogously we have

$$\int_{D_\Gamma^-} \mathcal{L}_v(f\mu) = \int_{\partial D_\Gamma^-} fi_v\mu$$

where $\partial D_\Gamma^+ = \Gamma$, $\partial D_\Gamma^- = -\Gamma$, so finally we get

$$\int_M \mathcal{L}_v^{\mathcal{R}}(f\mu) = \int_\Gamma \text{jump}(f)i_v\mu.$$

□

Now we can get the structure of the Lie algebroid $\text{DVect}(M) \rightarrow \text{V}(M)$ corresponding to the Lie groupoid $\text{DDiff}(M) \rightrightarrows \text{V}(M)$, adapted from [16, Theorem 6.5].

Theorem 3.5. *The Lie algebroid associated with the Lie groupoid $\text{DDiff}(M)$, denoted as $\text{DVect}(M)$, defines the structure of discontinuous vector fields on the manifold M . Below is the detailed structure of $\text{DVect}(M)$:*

1. *The fiber of $\text{DVect}(M)$ over Γ is the space $\text{DVect}(M, \Gamma)$ which consists of discontinuous vector fields of the form $u = \chi_\Gamma^+ u^+ + \chi_\Gamma^- u^-$, where χ_Γ^\pm are the indicator functions of the domain D_Γ^\pm , u^\pm are smooth vector fields on D_Γ^\pm , the normal component of u on Γ is continuous, i.e. $(u^+|_\Gamma - u^-|_\Gamma) // \Gamma$.*
2. *The anchor map $\# : \text{DVect}(M, \Gamma) \rightarrow T_\Gamma \text{V}(M)$ is given by the projection of $u^+|_\Gamma$ or $u^-|_\Gamma$ to their normal components, i.e. $\#u = \partial_t \Gamma$.*
3. *Let ζ, η be sections of $\text{DVect}(M)$, the algebroid bracket is defined as:*

$$[\zeta, \eta](\Gamma) = [\zeta(\Gamma), \eta(\Gamma)]^{\mathcal{R}} + \mathcal{L}_{\#\zeta(\Gamma)}\eta - \mathcal{L}_{\#\eta(\Gamma)}\zeta, \quad (3.5)$$

where $[u, v]^{\mathcal{R}}$ is the regularized Lie bracket:

$$[u, v]^{\mathcal{R}} = [\chi_\Gamma^+ u^+ + \chi_\Gamma^- u^-, \chi_\Gamma^+ v^+ + \chi_\Gamma^- v^-]^{\mathcal{R}} = \chi_\Gamma^+ [u^+, v^+] + \chi_\Gamma^- [u^-, v^-],$$

The derivative $\mathcal{L}_{\#\zeta(\Gamma)}\eta$ stands for the regularized derivative of η in the direction $\#\zeta(\Gamma_0)$:

$$\mathcal{L}_{\#\zeta(\Gamma)}\eta = \left. \frac{d^{\mathcal{R}}}{dt} \right|_{t=0} \eta(\Gamma_t),$$

Γ_t is any smooth curve with $\Gamma_0 = \Gamma$ and the tangent vector at Γ_0 given by $\#\zeta(\Gamma_0)$.

Proof. The proof follows a similar structure to Theorem 6.5 in [16]. \square

Remark 3.6. *The fibers of $\text{DVect}(M)$ over Γ are not closed under the Lie bracket of vector fields. Specifically, the regularized Lie bracket $[\zeta(\Gamma), \eta(\Gamma)]^{\mathcal{R}}$ does not belong to $\text{DVect}(M, \Gamma)$, even though both $\zeta(\Gamma)$ and $\eta(\Gamma)$ have continuous normal components. However, the terms $\mathcal{L}_{\#\zeta(\Gamma)}\eta$ and $\mathcal{L}_{\#\eta(\Gamma)}\zeta$, despite their discontinuous normal components, can rectify the discontinuity in the first term $[\zeta(\Gamma), \eta(\Gamma)]^{\mathcal{R}}$. This compensatory ensures that the algebroid bracket $[\zeta, \eta](\Gamma)$ is indeed an element of $\text{DVect}(M, \Gamma)$.*

3.3 The tangent space to the algebroid and its dual

In this subsection, we describe the tangent and dual spaces of the Lie algebroid $\text{DVect}(M)$. The construction of the tangent space closely follows that of [16], as it represents the space of possible accelerations for discontinuous velocity fields. However, the dual space differs due to the absence of the divergence-free condition, leading to a modified formulation.

This distinction in the dual space also affects the subsequent structures. In particular, the Poisson bracket on the dual algebroid and the Euler-Arnold equation for Lie groupoids, which are introduced in the following subsections, differ from those in [16], as they inherently involve the modified dual space. The specific definitions are provided below.

Definition 3.7 (Tangent space to the Lie algebroid). *Let $u_t = \chi_{\Gamma_t}^+ u_t^+ + \chi_{\Gamma_t}^- u_t^- \in \text{DVect}(M)$ be a smooth curve in the space $\text{DVect}(M)$. Then the tangent vector to u_t at $t = t_0$ is a pair $(v, \xi) \in \text{DVect}'(M, \Gamma_{t_0}) \oplus T_{\Gamma_{t_0}}V(M)$, defined by*

$$v = \left. \frac{d^{\mathcal{R}}}{dt} \right|_{t=t_0} u_t, \quad \xi = \left. \frac{d}{dt} \right|_{t=t_0} \Gamma_t, \quad (3.6)$$

where the space

$$\text{DVect}'(M, \Gamma) = \{ \chi_{\Gamma}^+ u^+ + \chi_{\Gamma}^- u^- \mid u^{\pm} \in \text{Vect}(D_{\Gamma}^{\pm}) \}$$

is the space of vector fields that are discontinuous at Γ , without the requirement for the normal components of the vector fields to be continuous at Γ .

Next, we consider the smooth dual space of the Lie algebroid $\text{DVect}(M)$, which can be viewed as the momentum space of a fluid with vortex sheets. Let

$$D\Omega^1(M) = \bigcup_{\Gamma \in V(M)} D\Omega^1(M, \Gamma), \quad (3.7)$$

$$DDense(M) = \bigcup_{\Gamma \in V(M)} DDense(M, \Gamma). \quad (3.8)$$

As the dual of $\text{DVect}(M)$, we define the dual vector bundle as follows:

Definition 3.8 (Dual of the Lie algebroid). *The smooth dual vector bundle $\text{DVect}(M)^*$ is the space*

$$\text{DVect}(M)^* := D\Omega^1(M) \otimes DDense(M), \quad (3.9)$$

where \otimes denotes the tensor product.

The pairing between a 1-form density $\tilde{m} \in \text{DVect}(M, \Gamma)^* = \text{D}\Omega^1(M, \Gamma) \otimes \text{DDense}(M, \Gamma)$ and a vector field $u \in \text{DVect}(M, \Gamma)$ is given by the following formula [17, 19]:

$$\langle \tilde{m}, u \rangle = \langle m \otimes \mu, u \rangle := \int_M (i_u m) \mu,$$

where μ is the volume form and m is a 1-form.

Next, we describe the tangent spaces of this dual.

Definition 3.9 (Tangent vector of a discontinuous 1-form). *Let $m_t = \chi_{\Gamma_t}^+ m_t^+ + \chi_{\Gamma_t}^- m_t^- \in \text{D}\Omega^1(M)$ be a smooth curve of 1-forms defined on the manifold M and discontinuous along the hypersurface Γ_t . Then, at time $t = t_0$, the tangent vector to m_t is a pair consisting of the following two components:*

$$\left. \frac{d\mathcal{R}}{dt} \right|_{t=t_0} m_t \in \text{D}\Omega^1(M, \Gamma_{t_0}), \quad \left. \frac{d}{dt} \right|_{t=t_0} \Gamma_t \in T_{\Gamma_{t_0}} \text{V}(M). \quad (3.10)$$

This structure allows us to describe the tangent space of $\text{DVect}(M)^*$. Given any $\tilde{m} \in \text{DVect}(M, \Gamma)^*$, its tangent space has a splitting

$$T_{\tilde{m}} \text{DVect}(M)^* \simeq \text{DVect}(M, \Gamma)^* \oplus T_{\Gamma} \text{V}(M). \quad (3.11)$$

To see this, let \tilde{m}_t be any smooth curve in $\text{DVect}(M)^*$ corresponding to the curve $\Gamma_t \in \text{V}(M)$, where $\Gamma_0 = \Gamma$ and $\tilde{m}_0 = m \otimes \mu$. Then, for this curve \tilde{m}_t , we can associate it with the following pair:

$$\left. \frac{d\mathcal{R}}{dt} \right|_{t=0} \tilde{m}_t \in \text{DVect}(M, \Gamma)^*, \quad \left. \frac{d}{dt} \right|_{t=0} \Gamma_t \in T_{\Gamma} \text{V}(M).$$

Then this correspondence establishes an isomorphism between $T_{\tilde{m}} \text{DVect}(M)^*$ and $\text{DVect}(M, \Gamma)^* \oplus T_{\Gamma} \text{V}(M)$.

3.4 Poisson bracket on the dual algebroid

First, we introduce the cotangent space to the base space $\text{V}(M)$, denoted as $T_{\Gamma}^* \text{V}(M)$, and then describe the cotangent space to the dual Lie algebroid $\text{DVect}(M)^*$, denoted as $T_{\tilde{m}}^* \text{DVect}(M)^*$.

Definition 3.10 (Cotangent space to the base space). *The cotangent space $T_{\Gamma}^* \text{V}(M)$ is the function space $C^\infty(\Gamma) \otimes \text{Dense}(\Gamma)$, where these functions are defined on the hypersurface Γ and take values in the density space. The pairing between $\tilde{f} \in C^\infty(\Gamma) \otimes \text{Dense}(\Gamma)$ and the highest-degree form $\xi \in T_{\Gamma} \text{V}(M) = \Omega^{n-1}(\Gamma)$ (where $n = \dim M$) is given by*

$$\langle \tilde{f}, \xi \rangle = \int_{\Gamma} f \xi.$$

Now, by dualizing the splitting (3.11), we obtain the cotangent space to the dual Lie algebroid $\text{DVect}(M)^*$.

Definition 3.11 (Cotangent space to the dual algebroid). *Let $\tilde{m} \in \text{DVect}(M, \Gamma)^*$. Then the smooth cotangent space of $\text{DVect}(M)^*$ at \tilde{m} is given by*

$$T_{\tilde{m}}^* \text{DVect}(M)^* = \text{DVect}(M, \Gamma) \oplus T_{\Gamma}^* \text{V}(M). \quad (3.12)$$

Furthermore, we define a differentiable function on the dual Lie algebroid $\text{DVect}(M)^*$. A function is differentiable if it has a differential belonging to the cotangent space, as follows:

Definition 3.12 (Differentiable function on the dual Lie algebroid). *A function $\mathcal{F} : \text{DVect}(M)^* \rightarrow \mathbb{R}$ is differentiable if there exists a section $d\mathcal{F}$ of the smooth cotangent bundle $T^*\text{DVect}(M)^*$ such that for any smooth curve \tilde{m}_t in $\text{DVect}(M)^*$, the following holds:*

$$\frac{d}{dt} \mathcal{F}(\tilde{m}_t) = \langle d\mathcal{F}(\tilde{m}_t), (\partial_t^R \tilde{m}_t, \partial_t \Gamma_t) \rangle. \quad (3.13)$$

Based on equation (3.12), the differential $d\mathcal{F}(\tilde{m})$ for $\tilde{m} \in \text{DVect}(M, \Gamma)^*$ can be decomposed as follows:

$$d\mathcal{F}(\tilde{m}) = (d^F \mathcal{F}(\tilde{m}), d^B \mathcal{F}(\tilde{m})),$$

where

$$d^F \mathcal{F}(\tilde{m}) \in \text{DVect}(M, \Gamma), \quad d^B \mathcal{F}(\tilde{m}) \in T_\Gamma^* \mathbb{V}(M) = C^\infty(\Gamma) \otimes \text{Dense}(\Gamma).$$

Thus, equation (3.13) can be expressed as

$$\frac{d}{dt} \mathcal{F}(\tilde{m}_t) = \langle d^F \mathcal{F}(\tilde{m}_t), \partial_t^R \tilde{m}_t \rangle + \langle d^B \mathcal{F}(\tilde{m}_t), \partial_t \Gamma_t \rangle. \quad (3.14)$$

We adapt and generalize the Poisson bracket formulation from [16, Theorem 6.25] to accommodate the compressible setting, retaining the structure of the original proof, as detailed in the following theorem.

Theorem 3.13 (Poisson bracket on the dual algebroid). *Let $\mathcal{F}_1, \mathcal{F}_2 : \text{DVect}(M)^* \rightarrow \mathbb{R}$ be differentiable functions, and assume that $d\mathcal{F}_i(\tilde{m}) = (d^F \mathcal{F}_i(\tilde{m}), d^B \mathcal{F}_i(\tilde{m})) = (v_i, \tilde{n}_i)$. Then their Poisson bracket is given by*

$$\begin{aligned} \{\mathcal{F}_1, \mathcal{F}_2\}(\tilde{m}) &= \mathcal{P}_{\tilde{m}}(d\mathcal{F}_1, d\mathcal{F}_2) \\ &= \mathcal{P}_{\tilde{m}}((v_1, \tilde{n}_1), (v_2, \tilde{n}_2)) \\ &= \int_M m([v_1, v_2]^{\mathcal{R}}) \mu + \int_\Gamma (n_2 - \text{jump}(i_{v_2} m)) i_{v_1} \mu - \int_\Gamma (n_1 - \text{jump}(i_{v_1} m)) i_{v_2} \mu. \end{aligned} \quad (3.15)$$

Proof. Suppose section A of $\text{DVect}(M)^*$ is an arbitrary extension of \tilde{m} such that $A(\Gamma) = \tilde{m}$, U_i is a section of $\text{DVect}(M)$ given by $U_i = d^F \mathcal{F}_i(A)$ such that $U_i(\Gamma) = d^F \mathcal{F}_i(A(\Gamma)) = d^F \mathcal{F}_i(\tilde{m})$. According to the definition of the Poisson bracket on the dual of a Lie algebroid [8, 16] and the algebroid bracket in equation (3.5), we can write

$$\begin{aligned} \{\mathcal{F}_1, \mathcal{F}_2\}(A(\Gamma)) &= \{\mathcal{F}_1, \mathcal{F}_2\}(\tilde{m}) \\ &= \langle \tilde{m}, [U_1, U_2](\Gamma) \rangle + \#U_1(\Gamma) \cdot (\mathcal{F}_2(A) - \langle A, U_2 \rangle) - \#U_2(\Gamma) \cdot (\mathcal{F}_1(A) - \langle A, U_1 \rangle) \\ &= \langle \tilde{m}, [U_1(\Gamma), U_2(\Gamma)]^{\mathcal{R}} \rangle + \#U_1(\Gamma) \cdot U_2 - \#U_2(\Gamma) \cdot U_1 + \#U_1(\Gamma) \cdot (\mathcal{F}_2(A) - \langle A, U_2 \rangle) \\ &\quad - \#U_2(\Gamma) \cdot (\mathcal{F}_1(A) - \langle A, U_1 \rangle) \\ &= \langle \tilde{m}, [U_1(\Gamma), U_2(\Gamma)]^{\mathcal{R}} \rangle + \langle \tilde{m}, \#U_1(\Gamma) \cdot U_2 \rangle - \langle \tilde{m}, \#U_2(\Gamma) \cdot U_1 \rangle \end{aligned}$$

$$\begin{aligned}
& + \#U_1(\Gamma) \cdot (\mathcal{F}_2(A) - \langle A, U_2 \rangle) - \#U_2(\Gamma) \cdot (\mathcal{F}_1(A) - \langle A, U_1 \rangle) \\
= & \langle \tilde{m}, [U_1(\Gamma), U_2(\Gamma)]^{\mathcal{R}} \rangle + \#U_1(\Gamma) \cdot (\mathcal{F}_2(A)) - \#U_1(\Gamma) \cdot \langle A, U_2 \rangle + \langle \tilde{m}, \#U_1(\Gamma) \cdot U_2 \rangle \\
& - (\#U_2(\Gamma) \cdot (\mathcal{F}_1(A)) - \#U_2(\Gamma) \cdot \langle A, U_1 \rangle + \langle \tilde{m}, \#U_2(\Gamma) \cdot U_1 \rangle) \\
= & \langle \tilde{m}, [U_1(\Gamma), U_2(\Gamma)]^{\mathcal{R}} \rangle + S_{12} - S_{21} \tag{3.16}
\end{aligned}$$

where

$$S_{12} = \#U_1(\Gamma) \cdot (\mathcal{F}_2(A)) - \#U_1(\Gamma) \cdot \langle A, U_2 \rangle + \langle \tilde{m}, \#U_1(\Gamma) \cdot U_2 \rangle, \tag{3.17}$$

$$S_{21} = \#U_2(\Gamma) \cdot (\mathcal{F}_1(A)) - \#U_2(\Gamma) \cdot \langle A, U_1 \rangle + \langle \tilde{m}, \#U_2(\Gamma) \cdot U_1 \rangle, \tag{3.18}$$

Now let's first compute S_{12} . Take any curve $\Gamma_1(t) \in V(M)$ such that $\Gamma_1(0) = \Gamma$, the tangent vector to $\Gamma_1(t)$ at Γ is $\#U_1(\Gamma)$, then

$$\begin{aligned}
\#U_1(\Gamma) \cdot (\mathcal{F}_2(A)) &= \nabla_{\#U_1(\Gamma)} \mathcal{F}_2(A) \\
&= \left. \frac{d}{dt} \right|_{t=0} \mathcal{F}_2(A(\Gamma_1(t))) \\
&= \left\langle d\mathcal{F}_2(A(\Gamma_1(t))), (\partial_t^R A(\Gamma_1(t)), \partial_t \Gamma_1(t)) \right\rangle \Big|_{t=0} \\
&= \left\langle (d^F \mathcal{F}_2(A(\Gamma_1(t))), d^B \mathcal{F}_2(A(\Gamma_1(t))), (\partial_t^R A(\Gamma_1(t)), \partial_t \Gamma_1(t))) \right\rangle \Big|_{t=0} \\
&= \left\langle d^F \mathcal{F}_2(A(\Gamma_1(t))), \partial_t^R A(\Gamma_1(t)) \right\rangle \Big|_{t=0} + \left\langle d^B \mathcal{F}_2(A(\Gamma_1(t))), \partial_t \Gamma_1(t) \right\rangle \Big|_{t=0} \\
&= \left\langle U_2(\Gamma), \left. \frac{d^R}{dt} \right|_{t=0} A(\Gamma_1(t)) \right\rangle + \langle d^B \mathcal{F}_2(\tilde{m}), \#U_1(\Gamma) \rangle. \tag{3.19}
\end{aligned}$$

Further, let $m_1(t)$ be any curve in $\Omega^1(M)$ lifting $A(\Gamma_1(t))$ and such that $m_1(0) = m$. Then using (3.3) we get

$$\begin{aligned}
\#U_1(\Gamma) \cdot \langle A, U_2 \rangle &= \nabla_{\#U_1(\Gamma)} \langle A, U_2 \rangle \\
&= \left. \frac{d}{dt} \right|_{t=0} \langle A(\Gamma_1(t)), U_2(\Gamma_1(t)) \rangle \\
&= \left. \frac{d}{dt} \right|_{t=0} \int_M i_{U_2(\Gamma_1(t))} m_1(t) \mu \\
&= \left. \frac{d^{\mathcal{R}}}{dt} \right|_{t=0} \int_M i_{U_2(\Gamma_1(t))} m_1(t) \mu + \int_{\Gamma_t} \text{jump}(i_{U_2(\Gamma_1(t))} m_1(t)) \frac{d\Gamma_1(t)}{dt} \Big|_{t=0} \\
&= \left. \frac{d^{\mathcal{R}}}{dt} \right|_{t=0} \langle A(\Gamma_1(t)), U_2(\Gamma_1(t)) \rangle + \int_{\Gamma} \text{jump}(i_{U_2(\Gamma)} m) \#U_1(\Gamma) \\
&= \left\langle \left. \frac{d^{\mathcal{R}}}{dt} \right|_{t=0} A(\Gamma_1(t)), U_2(\Gamma) \right\rangle + \left\langle \tilde{m}, \left. \frac{d^{\mathcal{R}}}{dt} \right|_{t=0} U_2(\Gamma_1(t)) \right\rangle + \int_{\Gamma} \text{jump}(i_{U_2(\Gamma)} m) \#U_1(\Gamma) \\
&= \left\langle \left. \frac{d^{\mathcal{R}}}{dt} \right|_{t=0} A(\Gamma_1(t)), U_2(\Gamma) \right\rangle + \langle \tilde{m}, \#U_1(\Gamma) \cdot U_2 \rangle + \int_{\Gamma} \text{jump}(i_{U_2(\Gamma)} m) \#U_1(\Gamma). \tag{3.20}
\end{aligned}$$

Substituting (3.19) and (3.20) into (3.17), we can get

$$S_{12} = \langle d^B \mathcal{F}_2(\tilde{m}), \#U_1(\Gamma) \rangle - \int_{\Gamma} \text{jump}(i_{U_2(\Gamma)} m) \#U_1(\Gamma), \tag{3.21}$$

Analogously we can get

$$S_{21} = \langle d^B \mathcal{F}_1(\tilde{m}), \#U_2(\Gamma) \rangle - \int_{\Gamma} \text{jump}(i_{U_1(\Gamma)} m) \#U_2(\Gamma), \quad (3.22)$$

Supposing $d\mathcal{F}_i(\tilde{m}) = (d^F \mathcal{F}_i(\tilde{m}), d^B \mathcal{F}_i(\tilde{m})) = (U_i(\Gamma), d^B \mathcal{F}_i(\tilde{m})) = (v_i, \tilde{n}_i)$, then

$$\begin{aligned} \{\mathcal{F}_1, \mathcal{F}_2\}(A(\Gamma)) &= \{\mathcal{F}_1, \mathcal{F}_2\}(\tilde{m}) = \mathcal{P}_{\tilde{m}}(d\mathcal{F}_1, d\mathcal{F}_2) \\ &= \mathcal{P}_{\tilde{m}}((v_1, \tilde{n}_1), (v_2, \tilde{n}_2)) \\ &= \langle \tilde{m}, [U_1(\Gamma), U_2(\Gamma)]^{\mathcal{R}} \rangle + S_{12} - S_{21} \\ &= \int_M m([v_1, v_2]^{\mathcal{R}}) \mu + \langle \tilde{n}_2, \#v_1 \rangle - \int_{\Gamma} \text{jump}(i_{v_2} m) \#v_1 \\ &\quad - \left(\langle \tilde{n}_1, \#v_2 \rangle - \int_{\Gamma} \text{jump}(i_{v_1} m) \#v_2 \right) \\ &= \int_M m([v_1, v_2]^{\mathcal{R}}) \mu + \int_{\Gamma} n_2 i_{v_1} \mu - \int_{\Gamma} \text{jump}(i_{v_2} m) i_{v_1} \mu \\ &\quad - \left(\int_{\Gamma} n_1 i_{v_2} \mu - \int_{\Gamma} \text{jump}(i_{v_1} m) i_{v_2} \mu \right) \\ &= \int_M m([v_1, v_2]^{\mathcal{R}}) \mu + \int_{\Gamma} \left(n_2 - \text{jump}(i_{v_2} m) \right) i_{v_1} \mu - \int_{\Gamma} \left(n_1 - \text{jump}(i_{v_1} m) \right) i_{v_2} \mu. \end{aligned}$$

□

Remark 3.14. As for the Lie-Poisson bracket on the dual Lie algebra \mathfrak{g}^* , it is defined as following [34]:

$$\{\mathcal{F}_1, \mathcal{F}_2\}(\tilde{m}) = \langle \tilde{m}, [d\mathcal{F}_1, d\mathcal{F}_2] \rangle = \langle \tilde{m}, [v_1, v_2] \rangle = \int_M m([v_1, v_2]) \mu, \quad \mathcal{F}_1, \mathcal{F}_2 \in C^\infty(\mathfrak{g}^*). \quad (3.23)$$

By comparing equation (3.15) and (3.23), we can see that the Poisson bracket on the dual Lie algebroid (3.15) is quite similar to the Lie-Poisson bracket on the dual Lie algebra (3.23) but with several boundary terms.

Corollary 3.15. Alternatively, the Poisson bracket can also be written in the following form:

$$\begin{aligned} \mathcal{P}_{\tilde{m}}((v_1, \tilde{n}_1), (v_2, \tilde{n}_2)) &= - \int_M d^{\mathcal{R}} m(v_1, v_2) \mu - \int_{\Gamma} n_1 i_{v_2} \mu + \int_{\Gamma} n_2 i_{v_1} \mu \\ &\quad - \int_M \text{div}^{\mathcal{R}}(v_1) i_{v_2} m \mu + \int_M \text{div}^{\mathcal{R}}(v_2) i_{v_1} m \mu. \end{aligned} \quad (3.24)$$

Proof. According to the Lemma 3.4 we have

$$\int_{\Gamma} \text{jump}(f) i_v \mu = \int_M (\mathcal{L}_v^{\mathcal{R}} f) \mu + \int_M \text{div}^{\mathcal{R}}(v) f \mu = \int_M \mathcal{L}_v^{\mathcal{R}}(f \mu), \quad (3.25)$$

then

$$\int_{\Gamma} \text{jump}(i_{v_2} m) i_{v_1} \mu = \int_M (\mathcal{L}_{v_1}^{\mathcal{R}} i_{v_2} m) \mu + \int_M \text{div}^{\mathcal{R}}(v_1) i_{v_2} m \mu,$$

$$\int_{\Gamma} \text{jump}(i_{v_1} m) i_{v_2} \mu = \int_M (\mathcal{L}_{v_2}^{\mathcal{R}} i_{v_1} m) \mu + \int_M \text{div}^{\mathcal{R}}(v_2) i_{v_1} m \mu.$$

By using the formula $i_{[v_1, v_2]} = [\mathcal{L}_{v_1}, i_{v_2}]$, then we obtain

$$\begin{aligned} & \mathcal{P}_{\tilde{m}}((v_1, \tilde{n}_1), (v_2, \tilde{n}_2)) \\ &= \int_M m([v_1, v_2]^{\mathcal{R}}) \mu + \int_{\Gamma} (n_2 - \text{jump}(i_{v_2} m)) i_{v_1} \mu - \int_{\Gamma} (n_1 - \text{jump}(i_{v_1} m)) i_{v_2} \mu \\ &= - \int_M d^{\mathcal{R}} m(v_1, v_2) \mu - \int_{\Gamma} n_1 i_{v_2} \mu + \int_{\Gamma} n_2 i_{v_1} \mu \\ &\quad - \int_M \text{div}^{\mathcal{R}}(v_1) i_{v_2} m \mu + \int_M \text{div}^{\mathcal{R}}(v_2) i_{v_1} m \mu. \end{aligned} \quad (3.26)$$

□

Remark 3.16. Unlike [16, Theorem 6.25], which applies to the divergence-free setting, the formulation (3.24) includes additional terms involving the divergence operator. This modification arises because we do not impose the divergence-free constraint, leading to a more general expression for the Poisson bracket that accounts for compressible cases. Furthermore, this distinction extends to the Hamiltonian operator introduced in the following Corollary 3.19, which significantly differs from its counterpart in [16].

Proposition 3.17. Let $\tilde{n} \in T_{\Gamma}^* V(M)(C^{\infty}(\Gamma) \otimes \text{Dense}(\Gamma))$. Then its image under the map $\#^* : T_{\Gamma}^* V(M) \rightarrow \text{DVect}(M, \Gamma)^*$ is given by

$$\#^* \tilde{n} := \{(d^{\mathcal{R}} h + T^{\mathcal{R}} h) \otimes \mu \mid \text{for any } h \in \text{DC}^{\infty}(M), \text{jump}(h) = n\}, \quad (3.27)$$

and the operator T is defined by the condition that $\int_M \text{div}^{\mathcal{R}}(v) f \mu = \langle T^{\mathcal{R}} f \otimes \mu, v \rangle$ for all $v \in \text{DVect}(M)$, $f \in \text{DC}^{\infty}(M)$.

Proof. Let $\tilde{n} \in T_{\Gamma}^* V(M)$, $v \in \text{DVect}(M, \Gamma)$, then we have

$$\langle \#^* \tilde{n}, v \rangle = \langle \tilde{n}, \#v \rangle = \int_{\Gamma} n i_v \mu. \quad (3.28)$$

By Lemma 3.4, for any $h \in \text{DC}^{\infty}(M)$ such that $\text{jump}(h) = n$, then we can rewrite the above integral as

$$\begin{aligned} \langle \#^* \tilde{n}, v \rangle &= \int_{\Gamma} n i_v \mu = \int_{\Gamma} \text{jump}(h) i_v \mu \\ &= \int_M (\mathcal{L}_v^{\mathcal{R}} h) \mu + \int_M \text{div}^{\mathcal{R}}(v) h \mu = \int_M (i_v d^{\mathcal{R}} h) \mu + \int_M \text{div}^{\mathcal{R}}(v) h \mu \\ &= \langle d^{\mathcal{R}} h \otimes \mu, v \rangle + \langle T^{\mathcal{R}} h \otimes \mu, v \rangle. \end{aligned}$$

Then we can get $\#^* \tilde{n} := (d^{\mathcal{R}} h + T^{\mathcal{R}} h) \otimes \mu$. □

Remark 3.18. If there is no sliding boundary, then it turns to the continuous case, so we have $\int_M \text{div}(v) f \mu = \langle -df \otimes \mu, v \rangle$, for all $v \in \text{Vect}(M)$, $f \in C^{\infty}(M)$.

Corollary 3.19. The Hamiltonian operator

$$\mathcal{P}_{\tilde{m}}^{\#} : T_{\tilde{m}}^* \text{DVect}(M)^* \rightarrow T_{\tilde{m}} \text{DVect}(M)^*$$

corresponding to the Poisson bracket on $DVect(M)^*$ is given by

$$(v, \tilde{n}) \mapsto ((-i_v d^{\mathcal{R}} m - \operatorname{div}^{\mathcal{R}}(v) \cdot m - d^{\mathcal{R}} i_v m) \otimes \mu + \#^* \widetilde{\operatorname{jump}(i_v m)} - \#^* \tilde{n}, \#v), \quad (3.29)$$

where $\#^* : T_{\Gamma}^* V(M) \rightarrow DVect(M, \Gamma)^*$ is the dual of the anchor map, explicitly given by

$$\#^* \tilde{n} := \{(d^{\mathcal{R}} h + T^{\mathcal{R}} h) \otimes \mu \mid \text{for any } h \in DC^{\infty}(M), \operatorname{jump}(h) = n\}. \quad (3.30)$$

Proof. To derive the explicit form of the Hamiltonian operator $\mathcal{P}_{\tilde{m}}^{\#}$ associated with the Poisson bracket on $DVect(M)^*$, we evaluate the pairing $\langle (v_2, \tilde{n}_2), \mathcal{P}_{\tilde{m}}^{\#}(v_1, \tilde{n}_1) \rangle$:

$$\begin{aligned} \langle (v_2, \tilde{n}_2), \mathcal{P}_{\tilde{m}}^{\#}(v_1, \tilde{n}_1) \rangle &= \mathcal{P}_{\tilde{m}}^{\#}((v_1, \tilde{n}_1), (v_2, \tilde{n}_2)) \\ &= - \int_M d^{\mathcal{R}} m(v_1, v_2) \mu - \int_M \operatorname{div}^{\mathcal{R}}(v_1) i_{v_2} m \mu + \int_M \operatorname{div}^{\mathcal{R}}(v_2) i_{v_1} m \mu \\ &\quad - \int_{\Gamma} n_1 i_{v_2} \mu + \int_{\Gamma} n_2 i_{v_1} \mu. \end{aligned}$$

Consider any $h \in DC^{\infty}(M)$ satisfying $\operatorname{jump}(h) = n_1$. This allows us to rewrite the boundary integral as follows:

$$\begin{aligned} \int_{\Gamma} n_1 i_{v_2} \mu &= \int_{\Gamma} \operatorname{jump}(h) i_{v_2} \mu \\ &= \int_M (\mathcal{L}_{v_2}^{\mathcal{R}} h) \mu + \int_M \operatorname{div}^{\mathcal{R}}(v_2) h \mu \\ &= \int_M (i_{v_2} d^{\mathcal{R}} h) \mu + \int_M \operatorname{div}^{\mathcal{R}}(v_2) h \mu. \end{aligned}$$

Substituting this into the Poisson bracket expression, we obtain

$$\begin{aligned} &\mathcal{P}_{\tilde{m}}^{\#}((v_1, \tilde{n}_1), (v_2, \tilde{n}_2)) \\ &= \int_M i_{v_2} (-i_{v_1} d^{\mathcal{R}} m) \mu - \int_M (i_{v_2} d^{\mathcal{R}} h) \mu - \int_M \operatorname{div}^{\mathcal{R}}(v_2) h \mu \\ &\quad + \int_{\Gamma} n_2 i_{v_1} \mu - \int_M \operatorname{div}^{\mathcal{R}}(v_1) i_{v_2} m \mu + \int_M \operatorname{div}^{\mathcal{R}}(v_2) i_{v_1} m \mu \\ &= \int_M i_{v_2} (-i_{v_1} d^{\mathcal{R}} m) \mu + \langle -\#^* \tilde{n}_1, v_2 \rangle + \int_{\Gamma} n_2 i_{v_1} \mu \\ &\quad + \int_M i_{v_2} (-\operatorname{div}^{\mathcal{R}}(v_1) m) \mu + \int_M \operatorname{div}^{\mathcal{R}}(v_2) i_{v_1} m \mu \\ &= \int_M i_{v_2} (-i_{v_1} d^{\mathcal{R}} m - \operatorname{div}^{\mathcal{R}}(v_1) \cdot m) \mu + \int_M \operatorname{div}^{\mathcal{R}}(v_2) i_{v_1} m \mu \\ &\quad + \langle -\#^* \tilde{n}_1, v_2 \rangle + \int_{\Gamma} n_2 i_{v_1} \mu \\ &= \int_M i_{v_2} (-i_{v_1} d^{\mathcal{R}} m - \operatorname{div}^{\mathcal{R}}(v_1) \cdot m) \mu + \left(- \int_M i_{v_2} d^{\mathcal{R}} i_{v_1} m \mu + \int_{\Gamma} \operatorname{jump}(i_{v_1} m) i_{v_2} \mu \right) \\ &\quad + \langle -\#^* \tilde{n}_1, v_2 \rangle + \int_{\Gamma} n_2 i_{v_1} \mu \\ &= \int_M i_{v_2} \left(-i_{v_1} d^{\mathcal{R}} m - \operatorname{div}^{\mathcal{R}}(v_1) \cdot m - d^{\mathcal{R}} i_{v_1} m \right) \mu + \int_{\Gamma} \operatorname{jump}(i_{v_1} m) i_{v_2} \mu \end{aligned}$$

$$\begin{aligned}
& + \langle -\#^* \tilde{n}_1, v_2 \rangle + \int_{\Gamma} n_2 i_{v_1} \mu \\
= & \left\langle \left(-i_{v_1} d^{\mathcal{R}} m - \operatorname{div}^{\mathcal{R}}(v_1) \cdot m - d^{\mathcal{R}} i_{v_1} m \right) \otimes \mu, v_2 \right\rangle + \left\langle \#^* \widetilde{\text{jump}}(i_{v_1} m), v_2 \right\rangle \\
& + \langle -\#^* \tilde{n}_1, v_2 \rangle + \int_{\Gamma} n_2 i_{v_1} \mu \\
= & \left\langle \left(-i_{v_1} d^{\mathcal{R}} m - \operatorname{div}^{\mathcal{R}}(v_1) \cdot m - d^{\mathcal{R}} i_{v_1} m \right) \otimes \mu + \#^* \widetilde{\text{jump}}(i_{v_1} m) - \#^* \tilde{n}_1, v_2 \right\rangle \\
& + \langle \# v_1, \tilde{n}_2 \rangle. \tag{3.31}
\end{aligned}$$

From (3.31), we could give an explicit formula about the Hamiltonian operator $\mathcal{P}_m^{\#}$ on $T_m^* \text{DVect}(M)^*$:

$$\mathcal{P}_m^{\#}((v, \tilde{n})) = \left(\left(-i_v d^{\mathcal{R}} m - \operatorname{div}^{\mathcal{R}}(v) \cdot m - d^{\mathcal{R}} i_v m \right) \otimes \mu + \#^* \widetilde{\text{jump}}(i_v m) - \#^* \tilde{n}, \# v \right). \tag{3.32}$$

□

Remark 3.20. *In the absence of sliding boundaries, it turns into a smooth and continuous case. In this case, the Lie groupoid $\text{DDiff}(M)$ reduces to the diffeomorphism Lie subgroup $G_V \subseteq \text{Diff}(M)$. The corresponding Hamiltonian operator $\mathcal{P}_m^{\#}$ on the cotangent space of the dual Lie algebra $T_m^* \text{Vect}(M)^*$ is given by*

$$\mathcal{P}_m^{\#}(v) = -(i_v dm + di_v m + \operatorname{div}(v)m) \otimes \mu.$$

3.5 Euler-Arnold equation for Lie groupoids

In this section, we deduce the extremal equations, namely the Euler-Arnold equations, for the Lie groupoid $\text{DDiff}(M) \rightrightarrows V(M)$. This derivation extends the framework developed in [16] for the incompressible setting by adapting it to the compressible case, where volume preservation and divergence-free conditions are no longer imposed. Consequently, the associated Euler-Arnold equations are modified accordingly.

Let $\mathcal{I} : \text{DVect}(M) \rightarrow \text{DVect}(M)^*$ be an inertia operator with a proper differential operator defined as $\mathcal{I}(u) = \mathcal{I}^{\mathcal{R}}(u) + \mathcal{I}_{\Gamma}(u)$, where $\mathcal{I}^{\mathcal{R}}$ is the regular part, acting withn each subdomain, and \mathcal{I}_{Γ} is an interface operator enforcing jump conditions across Γ , ensuring the self-adjointness of \mathcal{I} . The smooth dual space $\text{DVect}(M)^*$ of $\text{DVect}(M)$ can be generated by the \mathfrak{b} -map $\text{DVect}(M)^* := \{\mathcal{I}(u) : u \in \text{DVect}(M)\}$. Then for $u \in \text{DVect}(M, \Gamma)$, we have $\mathcal{I}(u) = u^{\mathfrak{b}} \otimes \mu = m \otimes \mu = \tilde{m}$, where $m = u^{\mathfrak{b}} \in \text{D}\Omega^1(M, \Gamma)$ and $u^{\mathfrak{b}}$ denotes the corresponding 1-form, and the inverse map is denoted by \sharp .

The inertia operator defines a metric on $\text{DVect}(M)$ given by the following: for $u, v \in \text{DVect}(M, \Gamma)$,

$$\langle u, v \rangle_{\text{DVect}(M, \Gamma)} := \langle \mathcal{I}(u), v \rangle = \langle m \otimes \mu, v \rangle = \int_M (i_v u^{\mathfrak{b}}) \mu = \int_M (i_v m) \mu. \tag{3.33}$$

The inverse of the inertia operator \mathcal{I} , where $\mathcal{I}^{-1}(\tilde{m}) = m^{\sharp} = u$, exists under proper conditions. In the smooth case, \mathcal{I}^{-1} is represented as a convolution with

a Green's function $v = G * \tilde{m}$. In the discontinuous case, \mathcal{I}^{-1} requires piecewise Green's functions for each subdomain, matched at Γ via interface conditions.

The inner product (3.33) defines a kinetic energy given by

$$H(v) = \frac{1}{2} \|v\|_{\text{DVect}(M,\Gamma)}^2 = \frac{1}{2} \langle v, v \rangle_{\text{DVect}(M,\Gamma)}. \quad (3.34)$$

Since the inertia operator is invertible, we can also define a dual metric on $\text{DVect}(M)^*$:

$$\begin{aligned} \langle \tilde{m}_1, \tilde{m}_2 \rangle_{\text{DVect}(M,\Gamma)^*} &:= \langle \mathcal{I}^{-1}(\tilde{m}_1), \tilde{m}_2 \rangle \\ &= \langle \mathcal{I}^{-1}(\tilde{m}_1), \mathcal{I}^{-1}(\tilde{m}_2) \rangle_{\text{DVect}(M,\Gamma)} \\ &= \langle u_1, u_2 \rangle_{\text{DVect}(M,\Gamma)} \end{aligned} \quad (3.35)$$

where \tilde{m}_1, \tilde{m}_2 belong to the same fiber in $\text{DVect}(M)^*$ with $\tilde{m}_1 = \mathcal{I}(u_1), \tilde{m}_2 = \mathcal{I}(u_2)$, yielding the corresponding Hamiltonian on $\text{DVect}(M)^*$:

$$H(\tilde{m}) = \frac{1}{2} \langle \tilde{m}, \tilde{m} \rangle_{\text{DVect}(M,\Gamma)^*}. \quad (3.36)$$

Remark 3.21. *An example of a self-adjoint inertia operator \mathcal{I} in the discontinuous setting is*

$$\mathcal{I}(u) = (\text{Id} - \Delta)^{\mathcal{R}} u + \mathcal{I}_\Gamma(u),$$

where the interface term is defined by

$$\langle \mathcal{I}_\Gamma(u), v \rangle = \int_\Gamma (v^+ \cdot (\nabla u^+ \cdot n) - v^- \cdot (\nabla u^- \cdot n)) \mu,$$

with homogeneous boundary conditions on ∂M .

Now we calculate the Euler-Arnold equations corresponding to the energy functional (3.34) under the metric (3.33) defined on $\text{DVect}(M)$.

Theorem 3.22 (Euler-Arnold equations on the dual Lie algebroid). *The Euler-Arnold equations for the energy functional (3.34) corresponding to the metric (3.33) on $\text{DVect}(M)$ written in terms of the 1-form density $\tilde{m} \in \text{DVect}(M)^*$ reads*

$$\begin{cases} \partial_t^{\mathcal{R}} \tilde{m} + (i_v d^{\mathcal{R}} m + \frac{1}{2} d^{\mathcal{R}} i_v m + \frac{1}{2} \text{div}^{\mathcal{R}}(v) \cdot m) \otimes \mu = 0, \\ \partial_t \Gamma = \#v, \end{cases} \quad (3.37)$$

where m is the 1-form, and $v = m^\sharp$ is the corresponding velocity field.

Proof. Since

$$H(\tilde{m}) = \frac{1}{2} \langle \tilde{m}, \tilde{m} \rangle_{\text{DVect}(M,\Gamma)^*} = \frac{1}{2} \langle v, \tilde{m} \rangle = \frac{1}{2} \int_M (m \cdot v) \mu.$$

let \tilde{m}_t be an arbitrary smooth curve in $\text{DVect}(M)^*$ with $\tilde{m}_{t=0} = \tilde{m}$, then using (3.3) we get

$$\left. \frac{d}{dt} \right|_{t=0} H(\tilde{m}_t) = \left. \frac{1}{2} \frac{d}{dt} \right|_{t=0} \int_M (m_t \cdot v_t) \mu$$

$$\begin{aligned}
&= \frac{1}{2} \frac{d^{\mathcal{R}}}{dt} \Big|_{t=0} \int_M (m_t \cdot v_t) \mu + \frac{1}{2} \int_{\Gamma_t} \text{jump}(m_t \cdot v_t) \frac{d\Gamma_t}{dt} \Big|_{t=0} \\
&= \left\langle v, \frac{d^{\mathcal{R}}}{dt} \Big|_{t=0} \tilde{m}_t \right\rangle + \left\langle \frac{1}{2} \text{jump}(m \cdot v) \otimes \text{Dense}(\Gamma), \frac{d\Gamma_t}{dt} \Big|_{t=0} \right\rangle.
\end{aligned} \tag{3.38}$$

According to the definition of the differential of a function in (3.14), we have

$$d^F H(\tilde{m}_t) = v, \quad d^B H(\tilde{m}_t) = \frac{1}{2} \text{jump}(m \cdot v) \otimes \text{Dense}(\Gamma).$$

Using the Poisson bracket on the dual Lie algebroid (3.31) and the Hamiltonian operator (3.29), we can get the Euler-Arnold equation in the dual Lie algebroid.

For this case, \tilde{n} in the equation (3.29) is $\tilde{n} = \frac{1}{2} \text{jump } i_v m \otimes \text{Dense}(\Gamma) = \frac{1}{2} \widetilde{\text{jump}(i_v m)}$, and h in the equation (3.30) is $h = \frac{1}{2} i_v m$, then according to the Proposition 3.17, we can get

$$\begin{aligned}
\left\langle \#^* \widetilde{\text{jump}(i_v m)} - \#^* \tilde{n}, v \right\rangle &= \left\langle \frac{1}{2} \widetilde{\text{jump}(i_v m)}, \#v \right\rangle \\
&= \frac{1}{2} \int_{\Gamma} \text{jump}(i_v m) i_v \mu \\
&= \frac{1}{2} \left(\int_M (\mathcal{L}_v^{\mathcal{R}} i_v m) \mu + \int_M \text{div}^{\mathcal{R}}(v) i_v m \mu \right) \\
&= \frac{1}{2} \left\langle (d^{\mathcal{R}} i_v m + \text{div}^{\mathcal{R}}(v) m) \otimes \mu, v \right\rangle,
\end{aligned} \tag{3.39}$$

so we can deduce that

$$\#^* \widetilde{\text{jump}(i_v m)} - \#^* \tilde{n} = \frac{1}{2} (d^{\mathcal{R}} i_v m + \text{div}^{\mathcal{R}}(v) m) \otimes \mu. \tag{3.40}$$

Then using the Hamiltonian operator (3.29), we have

$$\begin{aligned}
\mathcal{P}_m^{\#}((v, \tilde{n})) &= \left((-i_v d^{\mathcal{R}} m - \text{div}^{\mathcal{R}}(v) \cdot m - d^{\mathcal{R}} i_v m) \otimes \mu + \#^* \widetilde{\text{jump}(i_v m)} - \#^* \tilde{n}, \#v \right) \\
&= \left((-i_v d^{\mathcal{R}} m - \text{div}^{\mathcal{R}}(v) \cdot m - d^{\mathcal{R}} i_v m) \otimes \mu \right. \\
&\quad \left. + \frac{1}{2} (d^{\mathcal{R}} i_v m + \text{div}^{\mathcal{R}}(v) m) \otimes \mu, \#v \right) \\
&= \left((-i_v d^{\mathcal{R}} m - \frac{1}{2} \text{div}^{\mathcal{R}}(v) \cdot m - \frac{1}{2} d^{\mathcal{R}} i_v m) \otimes \mu, \#v \right).
\end{aligned} \tag{3.41}$$

So finally we get the Euler-Arnold equation on the dual Lie algebroid:

$$\begin{cases} \partial_t^{\mathcal{R}} \tilde{m} + (i_v d^{\mathcal{R}} m + \frac{1}{2} d^{\mathcal{R}} i_v m + \frac{1}{2} \text{div}^{\mathcal{R}}(v) \cdot m) \otimes \mu = 0, \\ \partial_t \Gamma = \#v. \end{cases} \tag{3.42}$$

□

3.6 Groupoid representation for discontinuous image registration

In this section, building on the groupoid representation theory introduced in the previous subsections, we extend the LDDMM method to address discontinuous image registration problems with sliding boundaries, resulting in an image registration method based on the discontinuous diffeomorphism Lie groupoid.

Specifically, consider two images $I_m : \Omega_m \rightarrow \mathbb{R}$ and $I_f : \Omega_f \rightarrow \mathbb{R}$ defined on the domains $\Omega_m \subset \mathbb{R}^2$ and $\Omega_f \subset \mathbb{R}^2$, where I_m is the moving image and I_f is the fixed image. Assume that the sliding boundary Γ is precomputed based on a prior segmentation on the space of the fixed image. The aim of discontinuous image registration is to find a reasonable discontinuous diffeomorphic deformation $\phi : \Omega_f \rightarrow \mathbb{R}^2$ such that warps the moving image to align it with the fixed image, i.e. $I_f \approx I_m^* = \phi \cdot I_m = I_m \circ \phi^{-1}$ [24]. In fact, given Γ , the registration problem seeks a discontinuous deformation $\phi = (\Gamma, \Gamma_1, \phi^+, \phi^-)$ located on the source fiber $\text{DDiff}(\Omega_f)_\Gamma$ corresponding to Γ .

Similar to the LDDMM method, we assume the deformation $\phi = \phi_{01}^v$ is obtained as the endpoint of a flow generated by the flow equation (2.2), and this deformation achieves the registration between the two images. The velocity $v : \Omega_f \rightarrow \mathbb{R}^2$ is located in the Lie algebroid $\text{DVect}(\Omega_f)$ corresponding to $\text{DDiff}(\Omega_f)$, and more specifically, it is located on the fiber $\text{DVect}(\Omega_f, \Gamma)$ at Γ . Therefore, to ensure the discontinuous deformation field is as simple as possible and as close as possible to the identity deformation Id_Γ , we use the metric defined in (3.33) on $\text{DVect}(\Omega_f)$. Thus, the regularization term for the deformation field can be defined as

$$E_R(\phi) = \min_{v(t) \in \text{DVect}(\Omega_f, \Gamma_0), \phi_{01}^v = \phi} \int_0^1 \|v(t)\|_{\text{DVect}(\Omega_f, \Gamma)}^2 dt.$$

Therefore, the registration method based on the discontinuous diffeomorphism Lie groupoid can be described as follows:

Definition 3.23 (Discontinuous Image registration based on Lie groupoid). *Given two images I_m and I_f defined on the domains Ω_m and Ω_f , respectively, and the sliding boundary Γ on the fixed image I_f , if a time-dependent vector field $v(t) (t \in [0, 1]) \in \text{DVect}(\Omega_f, \Gamma)$ can be found to minimize the following energy functional*

$$E(v) = E_S(\phi \cdot I_m, I_f) + \frac{1}{2} \int_0^1 \|v(t)\|_{\text{DVect}(\Omega_f, \Gamma)}^2 dt, \quad (3.43)$$

where ϕ_{0t}^v is the flow generated by $v(t)$, that is,

$$\partial_t \phi_{0t}^v(x) = v(t, \phi_{0t}^v(x)), \quad \phi_{00}^v(x) = x, \quad (3.44)$$

then $\phi = \phi_{01}^v$ is the optimal discontinuous diffeomorphic deformation to the discontinuous image registration problem.

Figure 1 illustrates the proposed framework of discontinuous image registration based on Lie groupoid and algebroid. Using the Euler-Arnold equations (3.37) derived in the previous subsection 3.5, we can obtain the solution to the optimization problem (3.43), thereby achieving the optimal discontinuous deformation.

Remark 3.24. *In the absence of a sliding boundary, the situation turns into a smooth and continuous case that is LDDMM. The Euler-Arnold equations (3.37) reduce to*

$$\partial_t \tilde{m} + (i_v dm + di_v m + \operatorname{div}(v)m) \otimes \mu = 0,$$

which is equivalent to the EPDiff equation in LDDMM (2.7): $\partial_t \tilde{m} + \mathcal{L}_v \tilde{m} = 0$.

4 Experiments

In this section, we test the proposed registration framework (3.43) and (3.44) on both synthetic examples and real lung images. The results in this section are specific to $d = 2$, and a three-dimensional implementation is an ongoing work. The experiments are implemented on the mermaid library (<https://github.com/uncbiag/mermaid>) that contains various image registration methods. The implementation is entirely written in Pytorch, leveraging its powerful automatic differentiation engine, which eliminates the need for manual gradient computation.

We test our proposed model on images exhibiting sliding motions and compare the results to those from registration with the Total Variation (TV) regularization [12], which also focuses on discontinuous registration and the LDDMM method. By including the TV method in our comparison, we aim to demonstrate the advantages and effectiveness of our proposed method compared to the existing method that tackles discontinuous registration differently. For both examples, the segmentations of the sliding boundaries are given by construction. For all experiments, we use the local normalized cross-correlation (LNCC) [3] as similarity measure due to its robustness to local intensity variations.

We first test our proposed model on synthetic rectangle images, which slide against each other: the upper region was moved to the right while the lower region was moved to the left, as shown in Figures 7(a) and 7(e). Figures 7(b) and 7(f) show the deformed moving image and deformed grid with the TV regularization. Although the TV method can capture the sliding motion, it produces unrealistic deformation as can be seen in Figure 7(f). Figures 7(c) and 7(g) show the deformed moving image and deformed grid with the LDDMM method. It is clear that the LDDMM produces incorrect motion estimates when sliding motion is present, as it produces smooth deformation thus resulting in a blurred boundary. In contrast, the proposed diffeomorphism groupoid method can effectively preserve the motion discontinuities at the sliding boundary, as shown in Figures 7(d) and 7(h).

The second evaluation was performed on a more complex sliding motion registration. The moving image was deformed by rotating the inner and outer circular regions by 5 degrees in opposite directions and then obtained the fixed image, as shown in Figures 8(a) and 8(e). When using the LDDMM method, the inner and outer parts are aligned smoothly as shown in Figures 8(c) and 8(g). In contrast, our proposed diffeomorphism groupoid method can accurately preserve the boundary and deal with the discontinuous deformation, as can be seen in Figures 8(d) and 8(h). Remarkably, our proposed method can achieve comparable results as the TV method, as shown in Figures 8(b) and 8(f).

To measure the quality of the registration, we consider the following quantities:

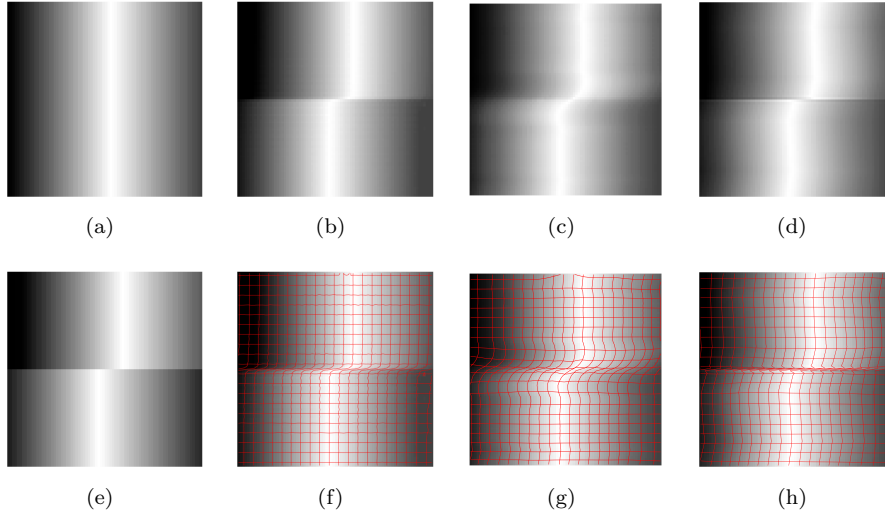


Figure 7: Registration results on synthetic rectangle images with sliding motion. (a) and (e) are the moving image and fixed image; (b)-(d) are the deformed moving images using TV, LDDMM, and the proposed diffeomorphism groupoid, respectively; (f)-(h) are the deformed grids obtained by TV, LDDMM, and the proposed diffeomorphism groupoid, respectively.

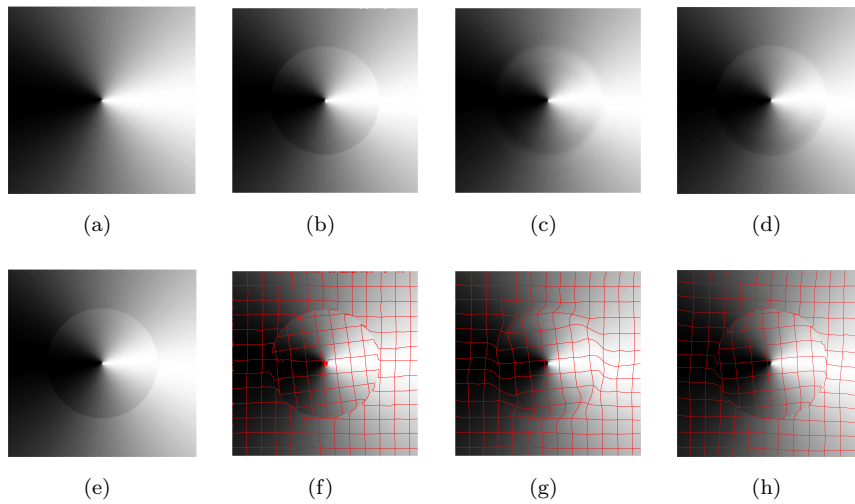


Figure 8: Registration results on synthetic wheel images with sliding motion. (a) and (e) are the moving image and fixed image; (b)-(d) are the deformed moving images using TV, LDDMM, and the proposed diffeomorphism groupoid, respectively; (f)-(h) are the deformed grids obtained by TV, LDDMM, and the proposed diffeomorphism groupoid, respectively.

Table 1: Comparison of $Re_SSD(\%)$, NCC and $SSIM$ by different methods. Bold values are the best values.

Data	Methods	$Re_SSD(\%)$	NCC	$SSIM$
Rectangle	Before	100	0.9228	0.8069
	TV	7.78	0.9949	0.9219
	LDDMM	10.98	0.9934	0.9396
	Proposed	6.25	0.9968	0.9755
Wheel	Before	100	0.9957	0.9690
	TV	61.09	0.9974	0.9720
	LDDMM	58.11	0.9975	0.9788
	Proposed	53.98	0.9977	0.9844

- Relative Sum of Squared Differences (Re_SSD) to measure the relative residual, which is defined by

$$Re_SSD = \frac{\|I_m^* - I_f\|^2}{\|I_m - I_f\|^2}$$

- Normalized Correlation Coefficient (NCC) is defined by

$$NCC(I_f, I_m^*) = \frac{\langle I_f - \bar{I}_f, I_m^* - \bar{I}_m^* \rangle}{\|I_f - \bar{I}_f\| \|I_m^* - \bar{I}_m^*\|},$$

$$\bar{I}_f = \frac{\int_{\Omega_f} I_f(\mathbf{x}) d\mathbf{x}}{|\Omega_f|}, \quad \bar{I}_m^* = \frac{\int_{\Omega_f} I_m^* d\mathbf{x}}{|\Omega_f|},$$

and $|\Omega_f|$ denotes the number of pixels in the fixed image domain.

- Structural Similarity ($SSIM$) [35] to evaluate the similarity of the images.

We summarize the evaluation results in Table 1 in a column in the order of Re_SSD , NCC , and $SSIM$ values for each method. From Table 1, we can see that the proposed method outperforms the LDDMM in terms of Re_SSD , NCC , and $SSIM$. This shows the effectiveness of the proposed discontinuous diffeomorphism groupoid method.

Finally, we evaluate the proposed method on real lung images, where sliding motion naturally occurs between lung tissues and the surrounding structures during breathing. For this experiment, the extreme inhale images are used as the fixed images, while the extreme exhale images serve as the moving images. The evaluation is performed on axial, coronal, and sagittal views, as shown in Figure 9, presented in rows from top to bottom. The fixed images are first segmented using the ITK SNAP program (<https://www.itksnap.org/>) to define the sliding boundaries, which serve as priors for the registration, and the proposed method is then used to estimate the deformation fields. The first and second columns in Figure 9 display the moving and fixed images, respectively, while the third and fourth columns show the residual difference images before and after registration using our proposed method. The last column shows the deformed moving images with deformation fields overlaid, in which the sliding boundaries are highlighted in yellow. The results demonstrate that our model

can handle the sliding motion effectively while preserving the structural consistency in homogeneous regions. This is particularly evident in the deformation fields shown within the green region of interest in Figures 9(e), 9(j) and 9(o), which demonstrate accurate preservation of discontinuities along the sliding boundaries.

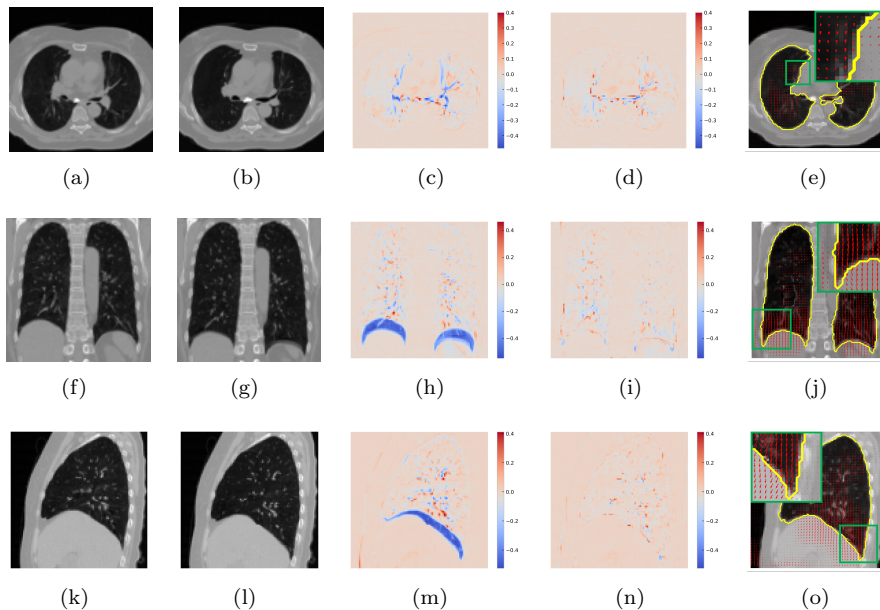


Figure 9: Registration results on real lung images with sliding motion. Rows from top to bottom display axial, coronal, and sagittal views. The first and second columns present the moving and fixed images, respectively. The third and fourth columns depict the residual difference images before and after registration obtained by the proposed method, respectively. The last column shows the deformed moving images by the proposed method with deformation fields overlaid, respectively, in which the sliding boundaries are shown in yellow.

5 Conclusions

In this paper, we have proposed a framework for discontinuous image registration by extending the classical diffeomorphism Lie group structure to a discontinuous diffeomorphism Lie groupoid. This new framework effectively handles discontinuities along the sliding boundary, addressing the limitation of traditional diffeomorphic registration methods. Moreover, a rigorous mathematical analysis of the associated structures including Lie algebroids and their duals is also provided. The extremal Euler-Arnold equations are derived to determine optimal flows for discontinuous deformations. Numerical tests show that the proposed model can achieve a satisfactory image registration result.

An accurate segmentation of the sliding boundary is crucial for our method, so developing an integrated method that simultaneously determines the location of the sliding boundary and performs registration is one of the main outlooks

of this work. Moreover, we plan to focus on extending the proposed model to 3D image registration for future research.

References

- [1] A. Izosimov and B. Khesin. Geometry of generalized fluid flows. *Calculus of Variations and Partial Differential Equations*, 63(1):3, 2024.
- [2] Vladimir Igorevich Arnold and Boris A Khesin. *Topological methods in hydrodynamics*, volume 19. Springer, 2009.
- [3] Asim Baig, M Ali Chaudhry, and Azhar Mahmood. Local normalized cross correlation for geo-registration. In *Proceedings of 2012 9th International Bhurban Conference on Applied Sciences & Technology (IBCAST)*, pages 70–74. IEEE, 2012.
- [4] Lili Bao, Ke Chen, Dexing Kong, Shihui Ying, and Tiejong Zeng. Time multiscale regularization for nonlinear image registration. *Computerized Medical Imaging and Graphics*, 112:102331, 2024.
- [5] Lili Bao, Jiahao Lu, Shihui Ying, and Stefan Sommer. Sliding at first-order: Higher-order momentum distributions for discontinuous image registration. *SIAM Journal on Imaging Sciences*, 17(2):861–887, 2024.
- [6] Martin Bauer, Stephen C Preston, and Justin Valletta. Liouville comparison theory for blowup of euler-arnold equations. *arXiv preprint arXiv:2306.09748*, 2023.
- [7] M Faisal Beg, Michael I Miller, Alain Trouvé, and Laurent Younes. Computing large deformation metric mappings via geodesic flows of diffeomorphisms. *International journal of computer vision*, 61:139–157, 2005.
- [8] Mohamed Boucetta. Riemannian geometry of lie algebroids. *Journal of the Egyptian Mathematical Society*, 19(1-2):57–70, 2011.
- [9] Noppadol Chumchob and Chen Ke. A variational approach for discontinuity-preserving image registration. *East-west Journal of Mathematics*, 2010:266–282, 2010.
- [10] Jean-Paul Dufour and Nguyen Tien Zung. *Poisson structures and their normal forms*, volume 242. Springer Science & Business Media, 2006.
- [11] Paul Dupuis, Ulf Grenander, and Michael I Miller. Variational problems on flows of diffeomorphisms for image matching. *Quarterly of applied mathematics*, pages 587–600, 1998.
- [12] Claudia Frohn-Schauf, Stefan Henn, and Kristian Witsch. Multigrid based total variation image registration. *Computing and Visualization in Science*, 11(2):101–113, 2008.
- [13] Yabo Fu, Shi Liu, H Harold Li, Hua Li, and Deshan Yang. An adaptive motion regularization technique to support sliding motion in deformable image registration. *Med. Phys.*, 45(2):735–747, 2018.

- [14] Darryl D Holm and Jerrold E Marsden. Momentum maps and measure-valued solutions (peakons, filaments, and sheets) for the epdiff equation. *The Breadth of Symplectic and Poisson Geometry: Festschrift in Honor of Alan Weinstein*, pages 203–235, 2005.
- [15] Darryl D Holm, Tanya Schmah, and Cristina Stoica. *Geometric Mechanics and Symmetry: From Finite to Infinite Dimensions*. Oxford University Press, USA, 2009.
- [16] Anton Izosimov and Boris Khesin. Vortex sheets and diffeomorphism groupoids. *Advances in Mathematics*, 338:447–501, 2018.
- [17] Boris Khesin, Gerard Misiołek, and Klas Modin. Geometric hydrodynamics and infinite-dimensional newton’s equations. *Bulletin of the American Mathematical Society*, 58(3):377–442, 2021.
- [18] Boris Khesin, Gerard Misiołek, and Alexander Shnirelman. Geometric hydrodynamics in open problems. *Archive for Rational Mechanics and Analysis*, 247(2):15, 2023.
- [19] Boris Khesin and Robert Wendt. *The geometry of infinite-dimensional groups*, volume 51. Springer Science & Business Media, 2008.
- [20] Andreas Mang and George Biros. Constrained h^1 -regularization schemes for diffeomorphic image registration. *SIAM J. Imaging Sci.*, 9(3):1154–1194, 2016.
- [21] Stephen Marsland and Stefan Sommer. Riemannian geometry on shapes and diffeomorphisms: Statistics via actions of the diffeomorphism group. In *Riemannian Geometric Statistics in Medical Image Analysis*, pages 135–167. Elsevier, 2020.
- [22] Mario Micheli, Peter W Michor, and David Mumford. Sobolev metrics on diffeomorphism groups and the derived geometry of spaces of submanifolds. *Izvestiya: Mathematics*, 77(3):541, 2013.
- [23] Michael I Miller, Alain Trouvé, and Laurent Younes. Geodesic shooting for computational anatomy. *Journal of mathematical imaging and vision*, 24:209–228, 2006.
- [24] Jan Modersitzki. *Numerical Methods for Image Registration*. Oxford University Press, New York, 2004.
- [25] David Mumford and Peter W Michor. On Euler’s equation and ‘EPDiff’. *Journal of Geometric Mechanics*, 5(3):319–344, 2013.
- [26] Francisco PM Oliveira and Joao Manuel RS Tavares. Medical image registration: a review. *Computer Methods in Biomechanics and Biomedical Engineering*, 17(2):73–93, 2014.
- [27] Xavier Pennec, Stefan Sommer, and Tom Fletcher. *Riemannian Geometric Statistics in Medical Image Analysis*. Academic Press, United Kingdom, 2019.

- [28] Laurent Risser, Habib Baluwala, and Julia A Schnabel. Diffeomorphic registration with sliding conditions: Application to the registration of lungs ct images. *Fourth International Workshop on Pulmonary Image Analysis, MICCAI*, pages 79–90, 2011.
- [29] Laurent Risser, François-Xavier Vialard, Habib Y Baluwala, and Julia A Schnabel. Piecewise-diffeomorphic image registration: Application to the motion estimation between 3d ct lung images with sliding conditions. *Med. Image Anal.*, 17(2):182–193, 2013.
- [30] Alexander Schmidt-Richberg, René Werner, Heinz Handels, and Jan Ehrhardt. Estimation of slipping organ motion by registration with direction-dependent regularization. *Med. Image Anal.*, 16(1):150–159, 2012.
- [31] Stefan Sommer, François Lauze, Mads Nielsen, and Xavier Pennec. Kernel bundle epdiff: evolution equations for multi-scale diffeomorphic image registration. In *Scale Space and Variational Methods in Computer Vision: Third International Conference, SSVM 2011, Ein-Gedi, Israel, May 29–June 2, 2011, Revised Selected Papers 3*, pages 677–688. Springer, 2012.
- [32] A. Trouvé. An infinite dimensional group approach for physics based models in patterns recognition. *Preprint*, 1995.
- [33] Max A Viergever, JB Maintz, Stefan Klein, Keelin Murphy, Marius Staring, and JPW Pluim. A survey of medical image registration-under review. *Medical Image Analysis*, 33:140–144, 2016.
- [34] Cornelia Vizman et al. Geodesic equations on diffeomorphism groups. *Symmetry, Integrability and Geometry: Methods and Applications*, 4:030, 2008.
- [35] Zhou Wang, Alan C Bovik, Hamid R Sheikh, and Eero P Simoncelli. Image quality assessment: from error visibility to structural similarity. *IEEE transactions on image processing*, 13(4):600–612, 2004.
- [36] Laurent Younes. *Shapes and Diffeomorphisms*. Springer, Berlin, Heidelberg, 2019.